Calhoun
Institutional Archive of the Naval Postgraduate School

Calhoun: The NPS Institutional Archive

DSpace Repository

Theses and Dissertations | 1. Thesis and Dissertation Collection, all items

1992-06

Microstructure and mechanical properties of high copper HSLA-100 steel in 2-inch plate form

Suka, Akira

Monterey, California. Naval Postgraduate School

http://hdl.handle.net/10945/23957

Copyright is reserved by the copyright owner

Downloaded from NPS Archive: Calhoun

http://www.nps.edu/library

Calhoun is the Naval Postgraduate School's public access digital repository for research materials and institutional publications created by the NPS community. Calhoun is named for Professor of Mathematics Guy K. Calhoun, NPS's first appointed -- and published -- scholarly author.

Dudley Knox Library / Naval Postgraduate School
411 Dyer Road / 1 University Circle
Monterey, California USA 93943

REPORT DOCUMENTATION PAGE

Form Approved
OMB No. 0704-0188

1a. REPORT SECURITY CLASSIFICATION UNCLASSIFIED	1b. RESTRICTIVE MARKINGS
2a. SECURITY CLASSIFICATION AUTHORITY	3. DISTRIBUTION /AVAILABILITY OF REPORT Approved for public release; distribution is unlimited.
2b. DECLASSIFICATION/DOWNGRADING SCHEDULE	
4. PERFORMING ORGANIZATION REPORT NUMBER(S)	5. MONITORING ORGANIZATION REPORT NUMBER(S)
6a. NAME OF PERFORMING ORGANIZATION Naval Postgraduate School 6b. OFFICE SYMBOL (*If applicable*) ME	7a. NAME OF MONITORING ORGANIZATION Naval Postgraduate School
6c. ADDRESS (*City, State, and ZIP Code*) Monterey, CA 93943	7b. ADDRESS (*City, State, and ZIP Code*) Monterey, CA 93943-5006
8a. NAME OF FUNDING/SPONSORING ORGANIZATION Naval Postgraduate School 8b. OFFICE SYMBOL (*If applicable*)	9. PROCUREMENT INSTRUMENT IDENTIFICATION NUMBER
8c. ADDRESS (*City, State, and ZIP Code*) Monterey, CA 93943	10. SOURCE OF FUNDING NUMBERS PROGRAM ELEMENT NO. / PROJECT NO. / TASK NO. / WORK UNIT ACCESSION NO.

11. TITLE (*Include Security Classification*)
Microstructure and Mechanical Properties of High Copper HSLA-100 Steel in 2-inch Plate Form

12. PERSONAL AUTHOR(S)
Suka, Akira

13a. TYPE OF REPORT	13b. TIME COVERED	14. DATE OF REPORT (*Year, month day*)	15. PAGE COUNT
Master's thesis	FROM_____TO_____	June, 1992	63

16. SUPPLEMENTARY NOTATION
The views expressed in this paper are those of the author and do not reflect the official policy or position of the Department of Defense or the U.S. Government.

17. COSATI CODES			18. SUBJECT TERMS (*Continue on reverse if necessary and identify by block number*)
FIELD	GROUP	SUB-GROUP	Steel, High Copper HSLA-100 Steel, mechanical property, microstructure

19. ABSTRACT (*Continue on reverse if necessary and identify by block number*)

The microstructure and mechanical properties of highly weldable high copper HSLA-100 steel in two-inch (50 mm) plate form were investigated in this work. The mechanical property data showed that the steel in the as-quenched and aged conditions not only met the mechanical property specifications of the Navy for HSLA (HY) 100 steels but also satisfied the requirements for HY-130 steels. Optical, scanning and transmission electron microscope studies of the as-quenched plate indicated that the microstructure was a mixture of lath martensite/retained austenite and bainitic ferrite, which is typical of these steels. On aging this microstructure developed the tempered structures usually encountered in HSLA steels. This investigation concludes that.

- Increased copper HSLA steel meets all the mechanical property specifications of Navy HSLA-100 ksi yield strength steel regardless of heat treatment and plate thickness (up to 50 mm thickness).
- High copper HSLA-100 steel in 50 mm plate form can fulfill all the mechanical property requirements of Navy 130 ksi yield strength steel with an appropriate temper.
- The microstructures formed with various heat treatments are consistent with the HSLA-100 CCT diagram.
- Increasing copper in HSLA-100 steel also increases the toughness as well as the strength, though the dynamics of this process are not clear.

20. DISTRIBUTION/AVAILABILITY OF ABSTRACT	21. ABSTRACT SECURITY CLASSICIATION	
[x] UNCLASSIFIED/UNLIMITED [ ] SAME AS RPT. [ ] DTIC USERS	UNCLASSIFIED	
22a. NAME OF RESPONSIBLE INDIVIDUAL A. Fox	22b. TELEPHONE (*Include Area Code*) (408) 646-2142	22c. OFFICE SYMBOL NS/Fx

DD Form 1473, JUN 86 *Previous editions are obsolete.* SECURITY CLASSIFICATION OF THIS PAGE
S/N 0102-LF-014-6603 UNCLASSIFIED

T258748

Approved for public release; distribution is unlimited

Microstructure and Mechanical Properties of High Copper HSLA-100 Steel in 2-inch Plate Form

by

Akira Suka
Lieutenant, Maritime Self Defense Force of Japan
BSME, Nihon University, Japan, 1981

Submitted in partial fulfillment of the
requirements for the degree of

MASTER OF SCIENCE IN ENGINEERING SCIENCE

From the

NAVAL POSTGRADUATE SCHOOL
June 1992

ABSTRACT

The microstructure and mechanical properties of highly weldable high copper HSLA-100 steel in two-inch (50 mm) plate form were investigated in this work. The mechanical property data showed that the steel in the as-quenched and aged conditions not only met the mechanical property specifications of the Navy for HSLA (HY) 100 steels but also satisfied the requirements for HY-130 steels. Optical, scanning and transmission electron microscope studies of the as-quenched plate indicated that the microstructure was a mixture of lath martensite/retained austenite and bainitic ferrite, which is typical of these steels. On aging this microstructure developed the tempered structures usually encountered in HSLA steels. This investigation concludes that.

- Increased copper HSLA steel meets all the mechanical property specifications of Navy HSLA-100 ksi yield strength steel regardless of heat treatment and plate thickness (up to 50 mm thickness).
- High copper HSLA-100 steel in 50 mm plate form can fulfill all the mechanical property requirements of Navy 130 ksi yield strength steel with an appropriate temper.
- The microstructures formed with various heat treatments are consistent with the HSLA-100 CCT diagram.
- Increasing copper in HSLA-100 steel also increases the toughness as well as the strength, though the dynamics of this process are not clear.

TABLE OF CONTENTS

I. **INTRODUCTION** **1**

A. INTRODUCTION 1

II. **BACKGROUND** **4**

A. INTRODUCTION TO HSLA STEEL 4

B. REVIEW OF HSLA STEELS 6

C. EFFECT OF ALLOYING ELEMENT ADDITIONS 9

D. ORIGINS OF STRENGTH 12

E. MICROSTRUCTURE 14

F. THE TEMPERING PROCESS 14

G. SCOPE OF PRESENT WORK 16

III. **EXPERIMENTAL PROCEDURE** **17**

A. MATERIAL 17

B. MECHANICAL PROPERTIES 18

C. MICROSCOPY 18

1. Optical Microscopy 18

2. Scanning Electron Microcopy 19

3. Transmission Electron Microscopy 19

D. MICROHARDNESS TESTING 20

IV. **RESULT AND DISCUSSION** **21**

A. MECHANICAL BEHAVIOR 21

B. MICROHARDNESS 25

The "Block" Sample....25
The "Bar" Sample....26
C. MICROSTRUCTURE....27
The "Block" Sample....27
The "Bar" Sample....27
1. As-quenched High Copper HSLA-100 Steel....28
2. 583°C Peak Aged High Copper HSLA-100 Steel....34
3. 593°C Aged High Copper HSLA-100 Steel....39
4. 621°C Over Aged High Copper HSLA-100 Steel....42
5. Transformation Product Packet Dimensions....44
V. SUMMARY....45
A. CONCLUSION....45
1. Mechanical Properties....45
2. Microhardness....45
3. Microstructure....45
B. RECOMMENDATIONS....46
APPENDIX....48
REFERENCES....51
INITIAL DISTRIBUTION LIST....54

LIST OF TABLES

TABLE 1. HSLA-100 STEEL MIL-S-24645A COMPOSITION....6

TABLE 2. CHEMICAL COMPOSITIONS OF HIGH STRENGTH STRUCTURAL STEELS....7

TABLE 3. TRENDS OF INFLUENCE ON THE ALLOYING ELEMENTS....11

TABLE 4. HIGH COPPER HSLA-100 STEEL LOT GLE COMPOSITION....17

TABLE 5. DTRC TENSILE TEST RESULTS FOR HIGH COPPER HLA-100, DTRC CODE GLE....18

TABLE 6. HY-130 STEEL STRENGTH AND TOUGHNESS REQUIREMENTS....24

TABLE 7. HSLA-100 DUCTILITY REQUIREMENTS....24

TABLE A-1. DTRC CHARPY V-NOTCH IMPACT ENERGY TEST DATA HIGH COPPER HSLA-100....48

TABLE A-2. DTRC CHARPY V-NOTCH IMPACT ENERGY TEST DATA HIGH COPPER HSLA-100....49

TABLE A-3. DTRC CHARPY V-NOTCH IMPACT ENERGY TEST DATA HIGH COPPER HSLA-100....49

TABLE A-4. DTRC CHARPY V-NOTCH IMPACT ENERGY TEST DATA HIGH COPPER HSLA-100....50

TABLE A-5. DTRC CHARPY V-NOTCH IMPACT ENERGY TEST DATA HIGH COPPER HSLA-100....50

LIST OF FIGURES

Figure 1. The Graville Diagram: Influence of Carbon Level and Carbon Equivalent on Susceptibility to HAZ Cracking of Steel Plate.....5

Figure 2. HSLA-100 Steel Continuous Cooling Transformation Diagram.....8

Figure 3. Fe-Cu Phase Diagram.....13

Figure 4. High Copper HSLA-100 Steel Lot GLE 0.2% Yield Strength and Ultimate Tensile Strength.....21

Figure 5. High Copper HSLA-100 Steel Lot GLE DBTT Behavior at Various Aging Temperatures.....23

Figure 6. High Copper HSLA-100 Steel Lot GLE Ductility: Variation of Elongation and Reduction of Area with Aging Temperature.....24

Figure 7. Vickers Hardness Number versus Through Thickness Direction in the As-quenched High Copper HSLA-100 50mm Plate.....25

Figure 8. Vickers Hardness Number versus Aging Temperature in the As-quenched High Copper HSLA-100 Steel Lot GLE.....26

Figure 9. Packet Size versus Through Thickness Direction in the As-quenched High Copper HSLA-100 50mm Plate.....27

Figure 10. Optical Micrograph of As-quenched Transformation Product Packets at the Top Surface of the "Block" Sample.....29

Figure 11. SEM Micrograph of As-quenched Transformation Product Packets at the Top Surface of the "Block" Sample.....29

Figure 12. Optical Micrograph of As-quenched Transformation Product Packets at the Center of the "Block" Sample.....30

Figure 13. SEM Micrograph of As-quenched Transformation Product Packets at the Center of the "Block" Sample.....30

Figure 14. TEM Image Showing Lath Martensite and Retained Austenite at Lath Boundaries 31

Figure 15. TEM Image Showing Lath Martensite and Retained Austenite at Lath Boundaries 31

Figure 16. TEM Image Showing Bainite Lath, Dislocation and Auto Tempered Carbide 32

Figure 17. TEM Image Showing Blocky Retained Austenite and Bainite 32

Figure 18. Diffraction Pattern Showing a [133] Crystallographic Zone Axis 33

Figure 19. Diffraction Pattern Showing a [133] Crystallographic Zone Axis 33

Figure 20. Optical Micrograph of 538°C Aged Transformation Product Packets 35

Figure . SEM Micrograph of 538°C Aged Transformation Product Packets 35

Figure 22. TEM Image Showing Tempered Lath Martensite Microstructure 36

Figure 23. TEM Image Showing Tempered Fe_3C Precipitates Decorating Dislocations 36

Figure 24. Diffraction Pattern Showing a [133] Crystallographic Zone Axis 37

Figure 25. TEM Image Showing Twin-like Structure 37

Figure 26. Diffraction Pattern Showing a Twin-like Crystallographic Zone 38

Figure 27. Mechanism of Martensite Transformation 38

Figure 28. Optical Micrograph of 593°C Aged Transformation Product Packets 40

Figure 29. SEM Micrograph of 593°C Aged Transformation Product Packets 40

Figure 30. TEM Image Showing Incoherent fcc Copper Precipitates Decorating Dislocation (Bright Field) 41

Figure 31. TEM Image Showing Incoherent fcc Copper Precipitates Decorating Dislocation (Dark Field) 41

Figure 32. Diffraction Pattern of [111] Pole Showing Evidence of $(FeM)_3C$ Type Carbide 42

Figure 33. Variation of Transformation Product Packet Size with Aging Temperature 43

Figure 34. Variation of Martensite Lath Width with Aging Temperature 44

I. INTRODUCTION

A. INTRODUCTION

The proliferation of welding rather than riveting as the primary method of joining steel necessitated the development of steels with low carbon content. The strength of the steel was maintained by increasing manganese, although no cognizance of the advantage of this in terms of toughness was yet recognized. Failure by brittle fracture of welded structures resulted in a recognition that impact or fracture toughness was essential, and thus the need for a log impact transition temperature became apparent. It was also recognized that a high yield-strength was more important than a high tensile-strength. Thus the carbon content was lowered further, and the manganese was maintained at high levels. By refinement of grain size, accomplished by Al additions, yield strength was increased from 225 to 300 MPa and the impact transition temperature was lowered to below 0°C. Further increases in yield strength were then achieved by precipitation hardening while still maintaining low carbon and high manganese contents in fine-grained compositions.

To achieve the increase in strength, the as-rolled condition was used, which was economically advantageous. The impact toughness was not as good as could be desired. However, because of the coarse grain size using low rolling finishing temperatures, a fine grain size was subsequently produced, which also maintained some degree of precipitation hardening. So it was through an evolutionary process that controlled rolled grain-refined,

precipitation-hardening high-strength low-allow (HSLA) steel first appeared. [Ref. 1:pp. 60-61]

The structural integrity of ships hull must be assured in the most extreme environment. Dynamic loads, particularly in the form of shock waves must be considered when assessing materials performance and fracture safety. The fracture safety of a naval vessel is addressed through the use of structural steels and the welding materials used in hull fabrication must demonstrate high fracture toughness and flaw tolerance for extreme service conditions. The high strength steels traditionally used in naval ship construction, HY-80 and HY-100, were certified to meet these requirements. However, the welding of the HY-series steels requires a number of fabrication controls to prevent post-weld cracking, which results in high fabrication costs. The Navy initiated the HSLA steel research and development program to reduce shipbuilding costs associated with welding HY steels. [Ref. 2:p. 2]

ASTM A710 grade A steel was evaluated as an HSLA-80 steel by the Navy. HSLA-80 steel was certified for use in surface ship structural construction following evaluation of its structural and welding properties [Ref. 3:p. 1435]. Significant reduction in hull fabrication costs were realized through the reductions in process controls and inspections [Ref. 4:p. 64]. It has been utilized in the construction of Ticonderoga-class cruisers, the new Arleigh Burke-class Destroyers, in some structures of the later Nimitz class aircraft carriers, and the Wasp-class amphibious assault ship [Ref. 2:p. 3].

Based on the success of the HSLA-80 steel program, the U.S. Navy developed a program for HSLA-100 steel. The purpose is replacing the HY-100 steel used in the advanced submarine non-pressure hull structure design

and in surface ship topside construction with a HSLA-100 steel, for the benefit of weight reduction [Ref. 4:p. 64]

Certification of HSLA-100 steel was completed in 1989 and the first major use was in the construction of the Nimitz-class Aircraft Carrier, USS John C. Stennis (CVN-74) [Ref. 4:p. 64]

HSLA steels are all characterized by low C(0.06% maximum). The steels contain Cu for precipitation strengthening. Ni is used for prevention of hot-shortness and improved low temperature toughness. Cu and Mo increase hardenability and add resistance to softening during aging. [Ref. 5:p. 242]

The microstructural basis for the strength and toughness properties of a high copper HSLA-100 steel, which achieves the 130ksi yield strength level in 19mm plate form, was investigated by LT. Harvey Allen Winters in 1991.

This thesis will utilize microstructural analysis to investigate the properties of strength and toughness in high copper HSLA-100 steel in two-inch plate (50 mm) form.

II. BACKGROUND

A. INTRODUCTION TO HSLA STEEL

High-strength, low-alloy steel (HSLA) was developed early in the 20th Century as engineers sought a method of producing steel that could meet the industrial demand for enhanced resistance to impact and greater fracture toughness. Until the advent of HSLA, steel was typically characterized by high percentage content of carbon, manganese and nickel.

As welding rather than riveting was widely adopted as a means of joining steel plate, a low-carbon steel became a pressing necessity. The strength of the alloy was maintained by increasing the percentage of manganese. Although manganese also produces the additional attribute of increased toughness, the early developers were not yet cognizant of this added advantage.

Weld failure due to brittle fracture became a critical factor in joining plate and the need for a low impact transition temperature as a means of increasing weld toughness became apparent. The need for high yield strength to accompany higher tensile strength was also recognized at this time. To accomplish their goals, engineers lowered the carbon content even further, while maintaining relatively high levels of manganese. Niobium, vanadium and titanium were also introduced into various alloys. [Ref. 7:pp. 60-61]

The properties which are most critical in plate applications are strength, toughness and weldability. Toughness refers to the minimum resistance of a metal to both ductile and brittle fracture. Weldability refers both to the inherent capacity of steel to be joined by the welding process and to the

characteristics of the final weld, especially in the heat-affected zone (HAZ). One of the major factors governing the weldability of a plate steel is the immunity of the HAZ to cold cracking, which may occur as delayed or underbead, cracking subsequent to the fusion process.

This problem was examined in some detail by Graville, and his results are shown in Figure 1. [Ref. 8:pp. 451-452]

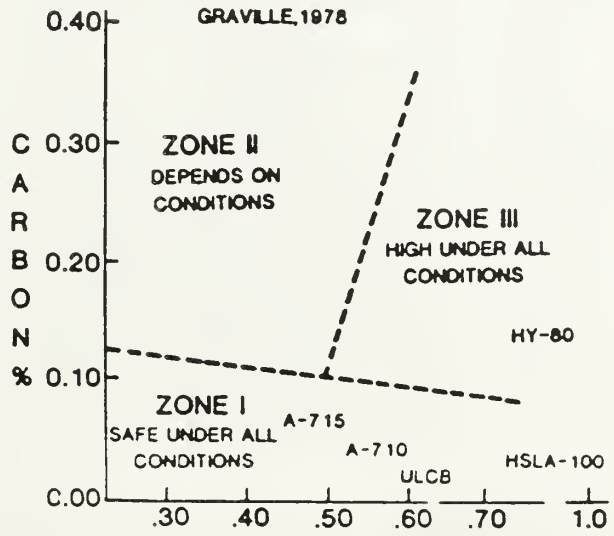

$$CE = C + \frac{Mn + Si}{6} + \frac{Ni + Cu}{15} + \frac{Cr + Mo + V}{5}$$

Figure 1. The Graville Diagram: Influence of Carbon Level and Carbon Equivalent on Susceptibility to HAZ Cracking of Steel Plate
[Ref. 9:p. 29]

As a means of weight reduction in ships and submarines, a significant tonnage of HY-100 steel has been used. A reduction in hull fabrication costs and higher productivity can be achieved by substitution of an HSLA steel for HY-100. The potential savings in manufacturing costs that can be realized by

using HSLA steel are attributable to the reduction or elimination of pre-heating the plate prior to welding [Ref. 4:p. 63].

The chemical composition of HSLA-100 steel according to MILSPEC MIL-S-24645A is listed in Table 1 [Ref. 11:p. 3].

TABLE 1. HSLA-100 STEEL MIL-S-24645A COMPOSITION (weight percent)

C	0.04-0.06
Mn	0.75-1.05
P	0.020
S	0.006
Si	0.40
Ni	3.35-3.65
Cr	0.45-0.75
Mo	0.55-0.65
Cu	1.45-1.75
Nb	0.02-0.06

B. REVIEW OF HSLA STEELS

HSLA-100 steel was developed as a replacement for HY-100 with the intent of reducing fabrication costs. The goal was to formulate an HSLA steel that would meet or exceed the strength and toughness of HY-100 steel and that was also weldable without preheating, using the same consumables and processes that were used in welding HY-100.

The specific composition ranges for HY-80, HY-100, HSLA-80 and HSLA-100 steels are compared in Table 2. Both HSLA-80 and HSLA-100 have an extra-low carbon content for enhanced weldability. HSLA-100 steel, however, has an increased alloy content when compared to HSLA-80. [Ref. 12:p. 2]

TABLE 2. CHEMICAL COMPOSITIONS OF HIGH STRENGTH STRUCTURAL STEELS
(Major elements for heavy gauge plate, greater than one inch)
[Ref. 2:P. 4] and [Ref. 7:p. 6]

Element (Wt. %)	Specific Chemical Composition			
	HY-80 MIL-S-1621K	HSLA-80 MIL-24645	HY-100 MIL-S-16216K	HSLA-100 MIL-S-24645A
C	0.13-0.118	0.06	0.15-0.20	0.06
Mn	0.10-0.40	0.40-0.70	0.10-0.40	0.75-1.05
p	0.015	0.202	0.015	0.020
S	0.008	0.006	0.008	0.006
Si	0.15-0.38	0.40	0.15-0.38	0.40
Ni	2.50-3.50	0.70-1.00	2.75-3.50	3.35-3.65
Cr	1.40-1.80	0.60-0.90	1.40-1.80	0.45-0.75
Mo	0.35-0.60	0.15-0.25	0.35-0.60	0.55-0.65
Cu	0.25	1.00-1.360	0.25	1.45-1.75
Nb	nil	0.02-0.06	nil	0.02-0.06

Alloy additions affect grain size, precipitation, solid solution strengthening, and the development of dislocation substructures. An increased copper content in steel (HSLA-Series) has moved the "nose" of proeutectoid ferrite (PF) transformation to the right on the Continuous Cooling Transformation Diagram (CCT).

Figure 2 represents a continuous cooling transformation diagram for HSLA-100 steel. [Ref. 13:p. 262]

In HSLA-100, the copper content has been made higher than in HSLA-80 for additional precipitation strengthening (maximum solubility of copper in iron is near two percent). An increase in strength was achieved by increasing the percentages of manganese, nickel, and molybdenum. Nickel, which was

increased the most in the new alloy, lowers upper shelf impact toughness and also lowers the impact toughness transition temperature. The microstructure of HSLA-100 steel has been identified with optical and scanning electron microscopy as being low-carbon martensite or bainite, depending on plate gauge. This is a significantly different metallurgy and microstructure than the ferritic HSLA-80 steel.

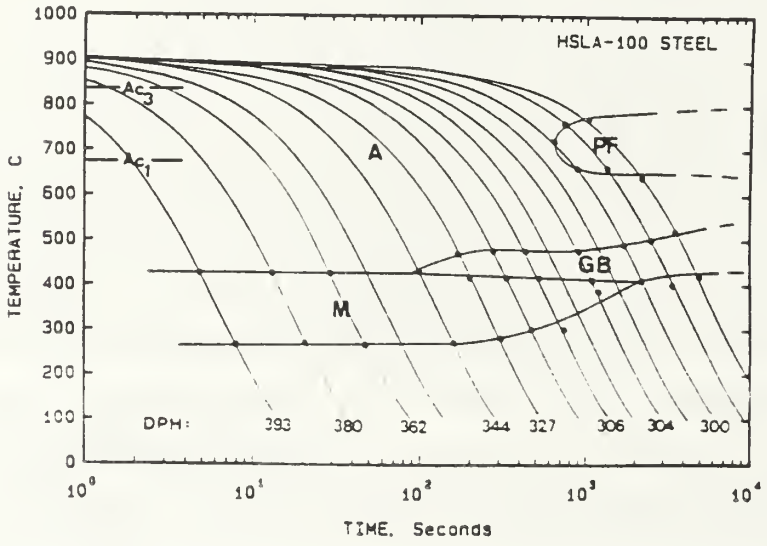

Figure 2. HSLA-100 Steel Continuous Cooling Transformation Diagram
[Ref. 13:p. 262]

One of the most desirable characteristics of the low-carbon, copper-strengthened HSLA steel is a weldment heat affected zone (HAZ) that has excellent strength and toughness. The primary reason for welding preheat is to mitigate underbead cracking (hydrogen related) in the hard, martensitic HAZ of HY steels. The HAZ of the HSLA steels typically does not harden but

may soften, due to the dissolution of copper and grain coarsening caused by the heat of welding. [Ref. 4:pp. 65-65]

The metallurgical significance of the alloying elements involved are listed below [Ref. 14:pp, 6-22 – 6-23].

C. EFFECT OF ALLOYING ELEMENT ADDITIONS

The percentage of an alloy element required for a given purpose ranges from a few hundredths of one percent to as high as five percent. The only way that an alloying element can affect the properties of the steel is to change the dispersion of carbide in the ferrite, change the properties of the ferrite, or change the properties of the carbide. The effect on the distribution of carbide is the most important factor, since in sections amenable to close control of structure, carbon steel is only moderately inferior to alloy steel. However, in large sections where carbon steels will fail to harden throughout the section even on a water quench, the hardenability of the steel can be increased by the addition of any alloying element (with the possible exception of cobalt). The increase in hardenability permits the hardening of a larger section of alloy steel than on plain carbon steel, and the quenching operation can be of diminished magnitude. Consequently, there is a smaller difference in temperature between the surface and center during quenching, and cracking and *warping* resulting from sharp temperature gradients in a steel during hardening can be avoided. The elements most effective in increasing the hardenability of steel are manganese, silicon, chromium, molybdenum, copper, and niobium.

Elements such as molybdenum, tungsten, chromium and vanadium are effective in increasing the hardenability when dissolved in the austenite, but these are often present in the form of carbides. They also prevent the agglomeration of carbides in tempered martensite. This is the main advantage of these carbide-forming elements. Tempering relieves the internal stresses in the hardened steel and causes spheroidization of the carbide particles with resultant loss in hardness and strength. The presence of these stable carbide-forming elements enables higher tempering temperatures to be used without a loss in strength. This imparts to these alloy steels the character of greater ductility for a given strength, or conversely, greater strength for a given ductility, than plain carbon steels.

The presence of alloying elements in the ferrite is the key to contribution of greater strength. Any element in solid solution in iron will increase its strength. The most effective elements for imparting greater strength have been found to be phosphorus, silicon, manganese, nickel, molybdenum, tungsten and chromium.

Another important effect of alloying elements is their influence on the austenitic grain size. Martensite formed from a fine-grained austenite has considerably greater resistance to shock than when formed from a coarse-grained austenite. The oxides formed by the deoxidation of the steel by different elements apparently prevent grain growth above the critical temperature over a considerable temperature range. To inhibit grain-growth, the most effective element is aluminum; most killed steels have some aluminum added during deoxidation. A similar effect on the austenite grain size results from the presence of finely scattered carbides in the austenite.

Elements forming stable carbides will also contribute to the formation of a fine-grained austenite. [Ref. 14:pp. 6-22]

Table 3 presents a summary of the effects of various alloying elements.

TABLE 3. TRENDS OF INFLUENCE ON THE ALLOYING ELEMENTS
[Ref. 14:pp. 6-22]

Element	As dissolved in ferrite, strength	As dissolved in austenite, hardenability	As undissolved carbide in austenite, fine grain toughness	As dispersed carbide in tempering high temp strength and toughness	As fine non-metallic dispersion, fine grain toughness
Al	moderate	mild	none	none	very strong
Cr	mild	strong	strong	moderate	slight
Co	strong	negative	none	none	none
Cb	little	strong	strong	strong	none
Cu	strong	moderate	none	none	none
Mn	strong	moderate	mild	mil	slight
Mo	moderate	strong	strong	strong	none
Ni	mild	mild	none	none	none
P	strong	mild	none	none	none
Si	moderate	moderate	none	none	moderate
Ta	moderate (?)	strong (?)	strong	strong	none
Ti	strong	strong	v.strong	little (?)	moderate
W	moderate	strong	strong	strong	none
V	mild	v.strong	v. strong	v. strong	moderate

The use of copper as an alloying element in low carbon HSLA steel has resulted in the following improvements: increased strength through precipitation of copper, while retaining toughness; greater weldability and formability, even at very low temperature; excellent corrosion resistance; production of lath bainitic/martensitic microstructures when used in conjunction with other microalloying elements; high fatigue strength and resistance to fatigue crack growth; suppression of hydrogen-induced cracking. The negative effect of added copper is the increased potential for *hot shortness* during hot working. [Ref. 15:p. 64]

High copper HSLA-100 is being investigated as a potential replacement for HY-130 steel. In research presently being done, it has been determined that the high copper alloy has a highly dislocated martensitic/bainitic microstructure. The martensitic microstructure is the major distinction between high copper HSLA-100 and HSLA steel. Though high copper HSLA-100 has a martensitic/bainitic microstructure, it is still highly weldable.

D. ORIGINS OF STRENGTH

Based on a comparison between HSLA and HY-130, the additional strengthening in HSLA appears to be derived through precipitation hardening of copper and a non-recrystallization controlled final roll pass. [Ref. 16:pp. 21-22] Coherent precipitation will result in a high degree of hardening due to the coherency of the strain fields associated with the interface of the steel matrix. The coherency of the strength fields will block dislocations and therefore lead to higher strength. Upon aging, the coherent precipitates become incoherent and their ability to block dislocation motion is reduced. Dislocation motion becomes easier and the material's strength begins to decrease [Ref. 17:pp. 319-324] The Fe-Cu phase diagram shown in Figure 3 shows that when cooling alloys of Fe containing Cu, three invariant reactions may be involved. Peritectic reactions at ~1484°C, and a eutectoid reaction at ~850°C. The products of the eutectoid reaction are ε-phase, i.e., FCC Cu with a small amount of Fe in solution and ferrite of α-phase Fe which contains a small quantity of Cu in solution. The maximum solubility of Cu in α-Fe is 2.1% at ~850°C. The decrease in solubility that coincides with a decrease in temperature provides the opportunity for subsequent precipitation or age hardening to be employed. [Ref. 18:pp. 6 and 8]

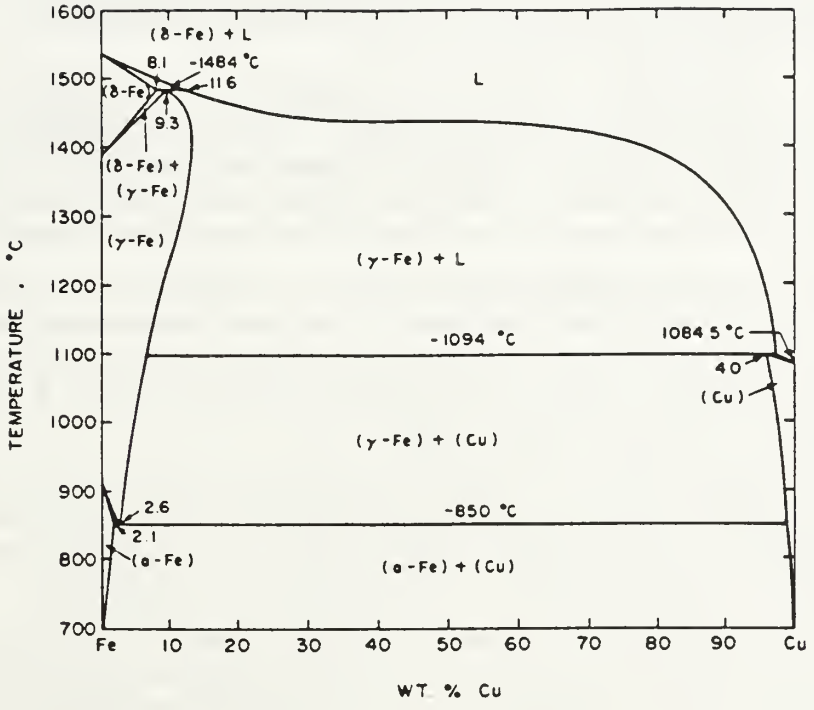

Figure 3. Fe-Cu Phase Diagram
[Ref. 18:p. 8]

It is possible to account for the strength of bainitic steels with four major mechanisms: [Ref. 7:p. 17]

- **Lath strengthening**. The relationship between strength and transformation product dimension is that flow stress varies with the reciprocal of lath length (lath dimension), width or colony/packet size.
- **Dislocation density.** The dislocation density of martensite and bainite is high. It has been observed by TEM. Higher dislocation density results in higher strength and the dislocation density has a relationship with the transformation temperature. The density varies with the reciprocal of the transformation temperature.
- **Interstitial and substitutional atom strengthening**. Solid solution strengthening was caused by dissolved carbon in the bainite ferrite. It was shown by experimental evidence that a residual super-saturation of carbon atoms can interact with dislocations to significantly increase the strength.

- **Carbide strengthening.** In upper bainite, the carbide particles formed at lath boundaries appear to prevent dislocation motion, thereby holding slip in the laths and increasing strength. A similar effect can be seen in lower bainite. There are also four major mechanisms of strength for high copper HSLA-100 steel.
- **Grain (packet) refinement.** In general, decreasing grain size is accompanied by increasing strength and by increasing ductility. This may explain why grain boundaries resist the passage of dislocations in a fine-grained material. There are more boundaries and hence more barriers, and the material is therefore stronger. [Ref 19:p. 661]
- **Solid solution strengthening.** When a foreign atom is introduced into a lattice, there is some distortion, which is more marked the greater the difference in the size between the foreign atom and the atoms of the parent lattice. Hence the foreign atom will act as a barrier to the passage of dislocation. [Ref. 20:p. 174]
- **Dislocation structure.** Phase transformations induce dislocations into the substructure, i.e. transformation from austenite to martensite. Deformation also induces dislocations within the substructure, for example: rolling below the recrystallization temperature.
- **Copper precipitation strengthening.** Incoherent ε-copper precipitates increase strengthening by impeding dislocation motion through Orowan looping [Ref. 18:p. 21-22]. The highest degree of hardening is caused by coherent precipitation. The coherent strain fields are made at their interface with the steel matrix. Coherent strain fields will block dislocation motion and result in higher strength.

E. MICROSTRUCTURE

The HSLA-100 steel continuous cooling transformation (CCT) diagram (Figure 2) suggests that a martensitic microstructure is to be expected in the surface region of an as-quenched sample and granular bainite, which consists of martensite and bainitic ferrite, is to be expected in the interior of the sample.

F. THE TEMPERING PROCESS

There are five stages of tempering for carbon or low-alloy steel.

Stage I Refrigeration, which usually converts much of the retained austenite to martensite, though the results are variable.

Stage II Heating in the range 200 to 400°F (95 to 204°C), in which (depending on the temperature) the martensite progressively loses its tetragonality to become cubic, and one finds the first precipitation of a "transition carbide" (not cementite).

Stage III Heating in the range 450 to 700°F (230 to 370°C), within which range the retained austenite is decomposed, being transformed, largely isothermally, to lower bainite (unless the retained austenite has previously been transformed to martensite by refrigeration).

Stage IV Tempering in the range 700 to 1000°F (370 to 540°C), causing formation of the cementite (Fe_3C) form of carbide.

Stave V Tempering in the range 1000 to 1300°F (540 to 705°C). In this range of temperature, there is merely further agglomeration of the cementite in plain carbon steel. But in alloy steels containing carbide-forming elements, tempering in this range causes the first formation of very finely dispersed alloy-rich carbides, believed to result from re-solution of cementite and contemporaneous precipitation of carbon as a special alloy-bearing carbide. This reaction often results in a marked retardation of the softening process—sometimes an actual increase in hardness—and is often designated as "secondary hardening."

[Ref. 21:p. 130]

There is another type of tempering, "auto-tempering" or "Q-tempering." This tempering occurs in steels with high martensite start temperatures and a carbon content of less than 0.2 weight percent. The precipitates have been identified as cementite (Fe_3C). [Ref. 22:p. 638] and [Ref. 23:p. 69]

In high copper HSLA-100 steel, auto-tempering will take place as a result of both the high martensite start temperature (~450°C) and the low carbon content. As it is quenched, the steel should go through the autotempering stage when small precipitates (Fe_3C) are formed. [Ref. 22:p. 638] and [Ref. 24]

G. SCOPE OF PRESENT WORK

The U.S. Navy and the David Taylor Research Center continue to investigate the HSLA series of steels which are certified to replace the HY series.

Previous work by Lt. Harvey A. Winters, which investigated the effect of increased copper on the HSLA-100 steel in 19.05mm plate, discussed the mechanical properties and microstructure at various aging temperatures.

In this work, the same steel and properties will be investigated in 50mm plate. Experimental data will be collected on the microhardness, mechanical properties and the microstructure. A change in the location of the proeutectoid ferrite region is anticipated due to the increased copper.

III. EXPERIMENTAL PROCEDURE

A. MATERIAL

A sample of high copper HSLA-100 plate steel with dimensions 2 inches in thickness, 7-1/2 inches in width and 9 inches in length was obtained from David Taylor Research Center (DTRC), Annapolis, Maryland, for this study. DTRC code GLE. It was manufactured by the Phoenix Steel Company. The block was heated to 900°C for two hours and then water quenched. A sample was then cut from the center of the block for the purpose of testing its hardness and observations of the microstructure. Five samples for quenching and aging were then made from the remaining portion of the bar. One was in the as-quenched form and the others were aged for one hour at the following temperatures: 538°, 566°, 593° and 621°C. Table 4 provides the chemical composition of the sample as determined by DTRC [Ref. 25:p. 14]

TABLE 4. HIGH COPPER HSLA-100 STEEL LOT GLE COMPOSITION

Element	Actual Composition
C	0.047
Mn	0.85
P	0.010
S	0.005
Si	0.22
Ni	3.59
Cr	0.57
Mo	0.60
Cu	2.00
Nb	0.025

B. MECHANICAL PROPERTIES

Data for the Charpy V-notch impact energy, ultimate tensile strength, 0.2% yield strength, percent reduction in area, and percent elongation were provided by DTRC [Ref. 25] The test data is listed in Table 5, and the Charpy test data is listed in Appendix A.

TABLE 5. DTRC TENSILE TEST RESULTS FOR HIGH COPPER HLA-100, DTRC CODE GLE

Aging Temperature (°C)	0.2% yield strength (KSI)	ultimate strength (KSI)	Percent elongation	% reduction in area	YS/UTS
as-quenched	95.3	151.0	18	66.5	0.64
538	138.5	140.0	22	66.0	0.95
566	135.5	140.5	23	68.5	0.96
593	128.5	132.0	24	72.0	0.97
621	120.0	123.0	24.5	74.0	0.98

C. MICROSCOPY

1. Optical Microscopy

Two types of metallographic samples were prepared. One was a "block" type and the other was a "bar" type. The block was used for the as-quenched sample and the bar type was used as the aging sample. Both samples were then progressively tempered at 538°, 566°, 593° and 621° and allowed one hour for aging.

One surface of the samples was polished using 240 grit, 320 grit, 400 grit, and 600 grit sandpaper. After polishing, the samples were washed with soap and water, cleaned with ethanol and blown dry.

The samples were then polished on a six micron polishing wheel with diamond paste. After polishing the samples were washed with soap and water, cleaned with ethanol and blown dry prior to polishing on the 0.5 micron polishing wheel with S_{10}. After polishing on the 0.5 micron polishing wheel, the samples were cleaned with soap and water again, cleaned with ethanol and blown dry. The samples were then etched with a four percent nital solution for approximately 10 seconds.

The polished and etched surfaces of the samples were examined at various magnifications (in a Zeiss ICM 405 photomicroscope). Photomicrographs were taken at 200X and 100X. For the "block" type sample photomicrographs were taken along the thickness direction from top to bottom at intervals of five millimeters. For the "bar" type sample, photomicrographs were taken near the top and bottom.

2. Scanning Electron Microcopy

Polished and etched samples were examined in a Cambridge Stereo Scan 5200 Scanning Electron Microscope. Micrographs were then taken at approximately 500X and 1000X. The micrographs were taken using secondary electron images and back-scattered electron images near the top and center of the sample.

3. Transmission Electron Microscopy

Discs were cut from the as-quenched, 538°, 566°, 593° and 621°C aging temperature samples using a low speed diamond wafer saw. The original cut produced discs of approximately 0.25mm in thickness. The samples were then thinned, using wet 200 grit sandpaper to thickness of approximately 0.18mm. Then, 320 grit wet sandpaper was used to thin the samples to

approximately 0.11 mm. The samples were then punched out to 3 mm diameter discs and thinned to approximately 0.05mm by using 400 grit wet sandpaper. The samples were then thinned to approximately 0.02mm thickness using wet 600 grit sandpaper.

The samples were subsequently thinned electrochemically, to perforation in a Struer's Tenupol electropolishing device operating at 70 volts and 0.5 amperes. The solution used was 3% perchloric acid, 62% ethanol, and 35% n-butoxy ethanol solution, which was cooled to approximately –20°C by liquid nitrogen. To remove redeposited copper on the sample, following the operation of electropolishing, a Gaton Dual Ion Mill (model 600) was used. The setting condition was 0.5 amperes and 5.0 kilovolts for 30 minutes at an angle of 15 degrees at room temperature. Following the ion milling a transmission electron microscope was utilized to investigate the microstructure of the sample. The transmission electron microscope (JEOL Model JEM 100CX) was operated at 120 kv.

D. MICROHARDNESS TESTING

The hardness distribution of the "block" sample was measured by a Micromet Microhardness Tester. The hardness of the sample taken from the "bar" was measured by the same method. A 200 gram weight was used to obtain the Vickers Hardness Number. The measurement of the "block" sample proceeded from the top to bottom surface at intervals of 1mm. The hardness test for the "bar" sample was taken at the center of the specimen. The testing procedure was duplicated fifteen times, with the final measurement determined by the mean value.

IV. RESULT AND DISCUSSION

A. MECHANICAL BEHAVIOR

The variation of ultimate tensile strength and 0.2% yield strength in relation to aging temperature are presented in Figure 4. The maximum value of ultimate tensile strength occurs at the as-quenched condition and then decreases as aging temperature increases. The maximum value of the 0.2% yield strength at 538°C also decreases as aging temperatures increase. This tendency is the result of the relationship between aging behavior and copper precipitation. [Ref. 26:p. 50]

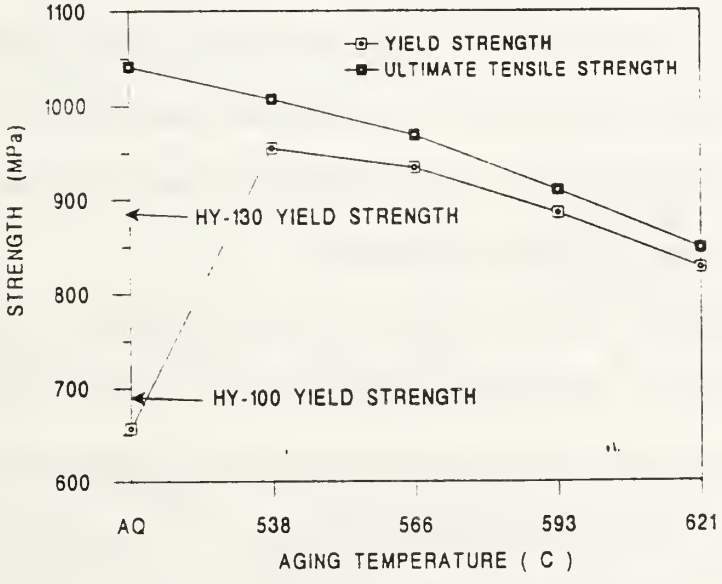

Figure 4. High Copper HSLA-100 Steel Lot GLE 0.2% Yield Strength and Ultimate Tensile Strength

The samples which were subjected to various aging temperatures including the as-quenched condition, were tested with the Charpy v-notch impact test at five different test temperatures. These were –84°C, –62°C, –40°C, –18°C and 25°C. Figure 5 shows the results of the impact test. We can see from the data presented on the graph that the impact energy increases as test temperature was increased. The relationship between aging temperature and impact energy displays a tendency for higher aging temperatures producing higher impact energy. The trend of both ultimate tensile strength and 0.2% yield strength is opposite to that of impact strength. The effect of aging temperature on impact energy is very pronounced. The impact energy at an aging temperature of 621°C is more than twice that at the temperature of 538°C.

There are two parameters to determine the value of ductility. These are the percentage of reduction in area and the percentage of elongation. Figure 6 represents both the percentage reduction in area and the percentage of elongation in relation to aging temperature.

The elongation of the sample varied between 18 percent (as quenched) and 24.5% for the 621°C tempered sample, while reduction in area increased with increase from 66% to 74% in the aging temperature.

The results of mechanical testing of lot GLE show that the samples which were aged at 621°C, 593°C and as-quenched satisfy the requirements of the Charpy v-notch impact toughness and percentage of elongation for HY-130 steel, but would not satisfy the requirement of 0.2% yield strength for HY-

130 steel. Both samples that were aged at 566°C and 538°C satisfied the requirement of 0.2% yield strength and elongation percent for HY-130 steel, but just about satisfied the requirement of the Charpy v-notch impact toughness for HY-130 steel. All the samples did satisfy the ductility requirements for HSLA-100 steel. These requirements are shown in Tables 6 and 7.

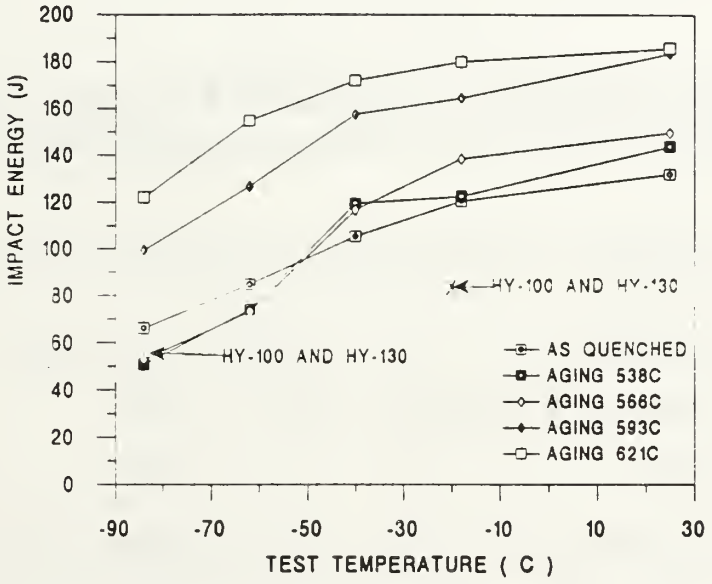

Figure 5. High Copper HSLA-100 Steel Lot GLE DBTT Behavior at Various Aging Temperatures

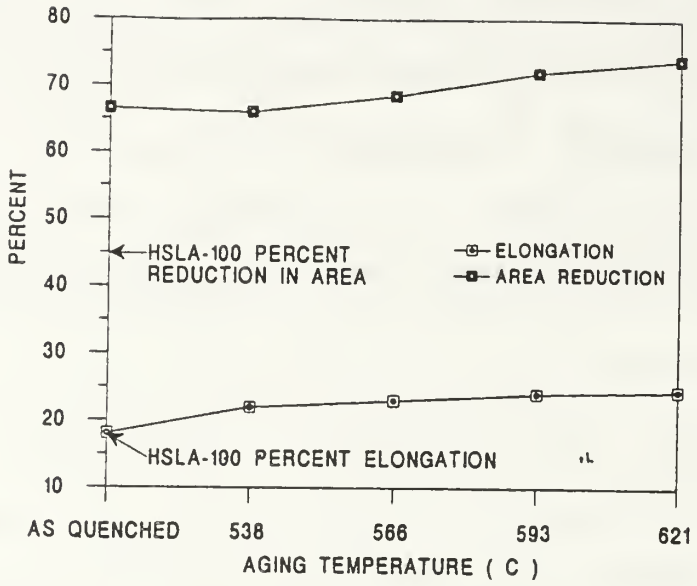

Figure 6. High Copper HSLA-100 Steel Lot GLE Ductility: Variation of Elongation and Reduction of Area with Aging Temperature

TABLE 6. HY-130 STEEL STRENGTH AND TOUGHNESS REQUIREMENTS

0.2% YIELD STRENGTH	896 MPa minimum
TRANSVERSE CHARPY V-NOTCH IMPACT TOUGHNESS	81.3J at –19°C 54.2J at –84°C
PERCENT ELONGATION	15% minimum in 50.8 mm

TABLE 7. HSLA-100 DUCTILITY REQUIREMENTS

PERCENT ELONGATION	18% minimum in 50.8 mm
PERCENT REDUCTION IN AREA	45% minimum

According to the mechanical property data obtained through testing by the DTRC, the best combination of strength and toughness occurs between

the aging temperatures of 566°C and 593°C. The microstructure of the samples which were aged 566°C and 621°C will be investigated in the present work. Both the over-aged condition (621°C) and the as-quenched condition will also be examined.

B. MICROHARDNESS

The "Block" Sample

A Vickers microhardness measurement was taken on an as-quenched specimen, 50 mm thick, that originated from the "block" sample. The results are shown in Figure 7.

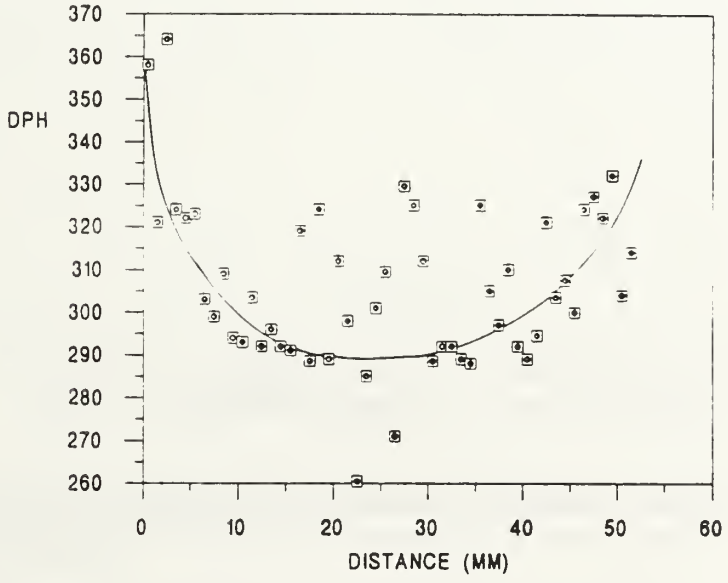

Figure 7. Vickers Hardness Number versus Through Thickness Direction in the As-quenched High Copper HSLA-100 50mm Plate

The test results indicated that the surface of the plate contained mostly martensite and a very small amount of retained austenite. This was inferred from an examination of the CCT diagram (Figure 2) The center of the plate

contained bainitic ferrite and also lath martensite and the fraction of bainitic ferrite was greater than that of martensite and retained austenite.

The "Bar" Sample

The microhardness of the center of the "bar" sample was measured. Figure 8 represents the relationship between the Vickers hardness test and aging temperature. The test results showed that the hardness decreased rapidly between 566°C and 593°C then increased from 593°C to 621°C. This phenomenon is related to the effects of the age hardening copper precipitates.

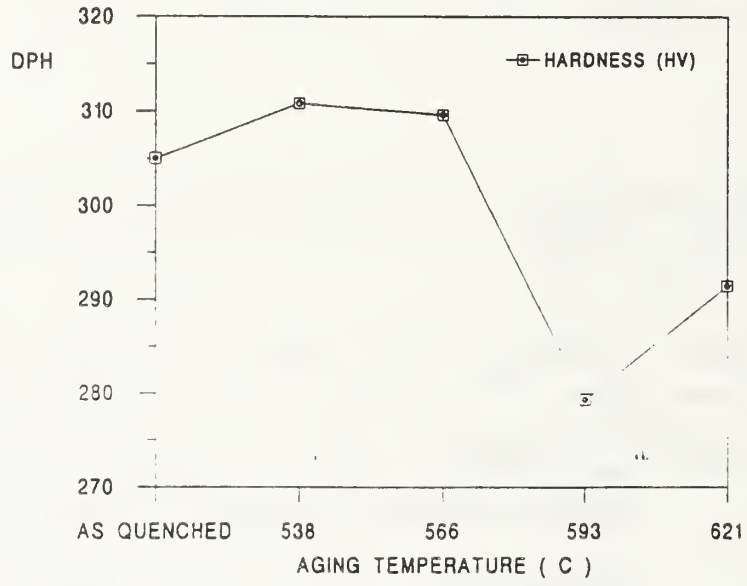

Figure 8. Vickers Hardness Number versus Aging Temperature in the As-quenched High Copper HSLA-100 Steel Lot GLE

C. MICROSTRUCTURE

The "Block" Sample

The surface of the "block" sample was observed by optical microscope. Measurement of the "packet" sizes were taken from the micrograph and the results are shown in Figure 9.

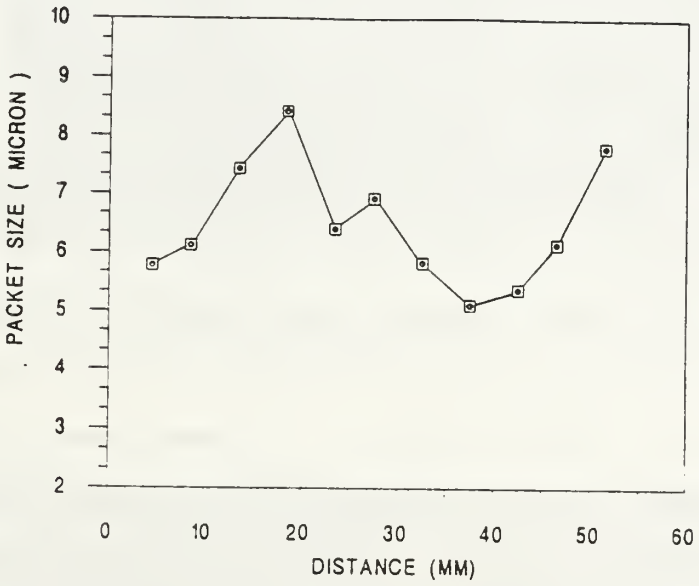

Figure 9. Packet Size versus Through Thickness Direction in the As-quenched High Copper HSLA-100 50mm Plate

The smallest dimension was 5.10 (μm) and the largest was 8.41 (μm).

The "Bar" Sample

All the "bar" samples (as-quenched, 538°C, 566°C, 593°C, and 621°C) were examined by transmission electron microscopy, optical microscopy, and scanning electron microscopy. The characteristics of the microstructure in each sample was analyzed in relationship to their mechanical properties.

1. As-quenched High Copper HSLA-100 Steel

The microstructure of the as-quenched high copper HSLA-100 steel sample was investigated with the optical microscope, SEM and TEM. The investigation showed that the transformation produced lath martensite, retained austenite and bainite. Figures 10 and 11 are representations of the optical and SEM micrographs taken from the top surface of the "block" sample. Figures 12 and 13 represent optical and SEM micrographs taken from the center of the "block" sample. A comparison of the two microstructures shows that the fraction of bainite is greater in the center than in the surface and that no proeutectoid ferrite was present at the center.

The general microstructure of lath martensite/bainite, obtained from the TEM micrographs are represented in Figures 14 and 15. These show the packet boundary, which consists of bainitic ferrite, martensite and retained austenite. Autotempered carbides (Fe_3C) and the high dislocation density in the bainite lath are shown in Figure 16. Retained austenite and bainite are presented in Figure 17. Autotempered carbide precipitates were observed and presented in Figures 18 and 19. An analysis of the observations show that the strength of the as-quenched HSLA-100 steel consists of the fine transformation product packet size, high dislocation density and small lath width. The fine transformation product packet size and high dislocation density results in greater strength while the fine martensitic laths contribute to toughness.

The findings and analysis of these observations are consistent with those previously reported by Howell pursuant to the investigation of oil-quenched HSLA-100 steel, and Winters in the investigation of water-quenched 19mm HSLA-100 steel. [Ref. 19:p. 34]

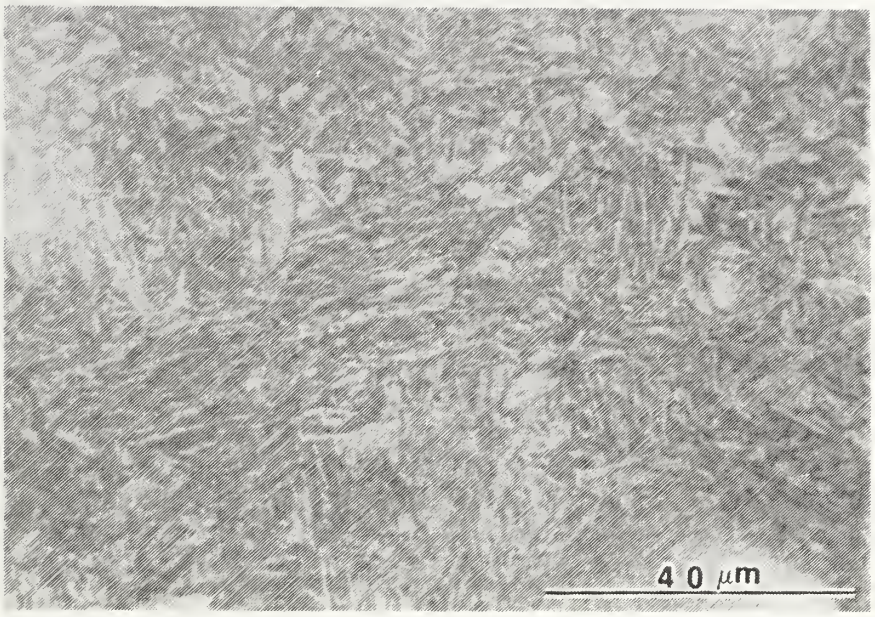

Figure 10. Optical Micrograph of As-quenched Transformation Product Packets at the Top Surface of the "Block" Sample

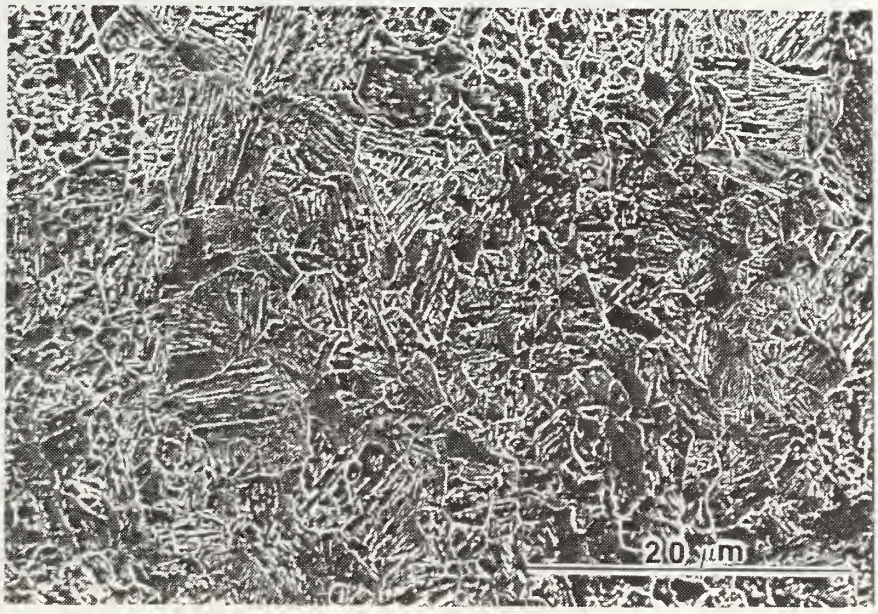

Figure 11. SEM Micrograph of As-quenched Transformation Product Packets at the Top Surface of the "Block" Sample

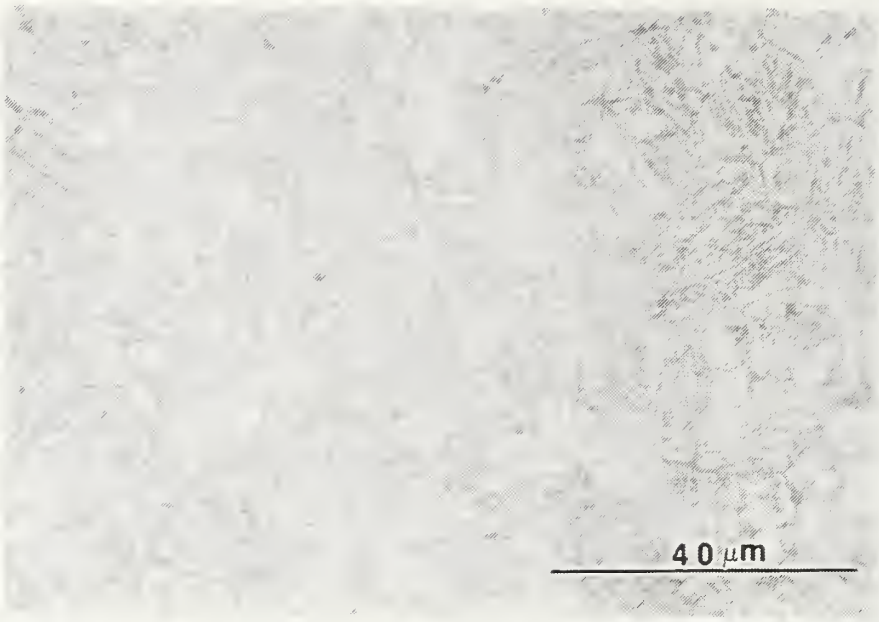

Figure 12. Optical Micrograph of As-quenched Transformation Product Packets at the Center of the "Block" Sample

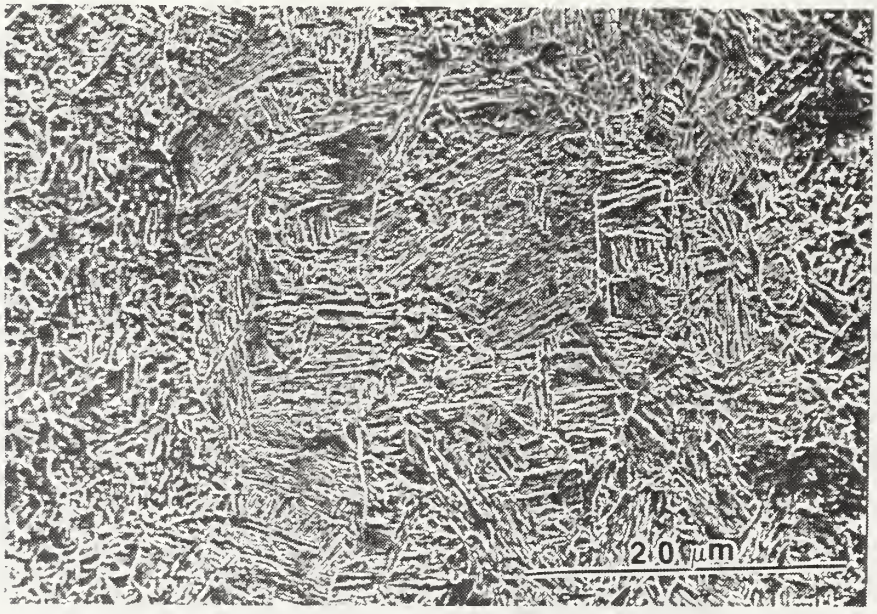

Figure 13. SEM Micrograph of As-quenched Transformation Product Packets at the Center of the "Block" Sample

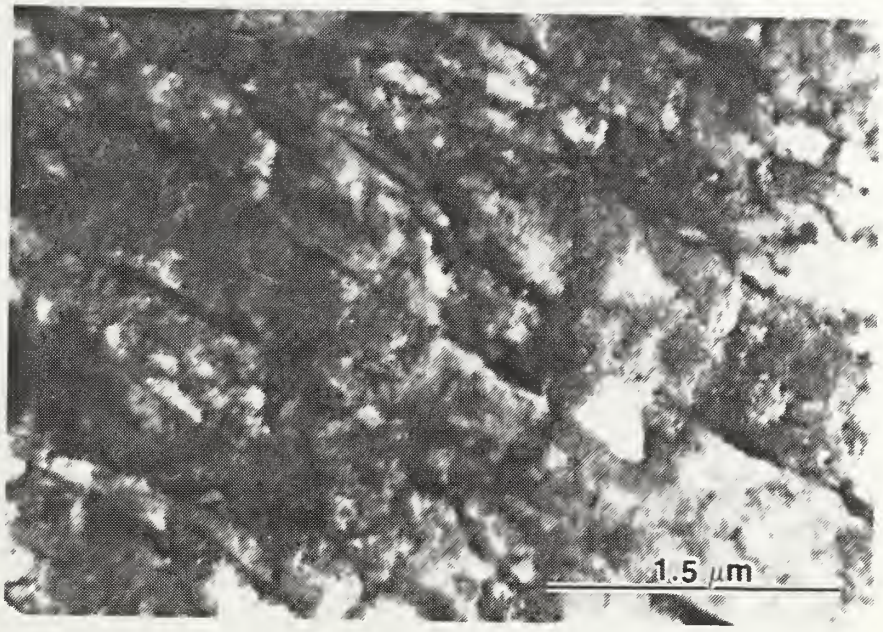

Figure 14. TEM Image Showing Lath Martensite and Retained Austenite at Lath Boundaries

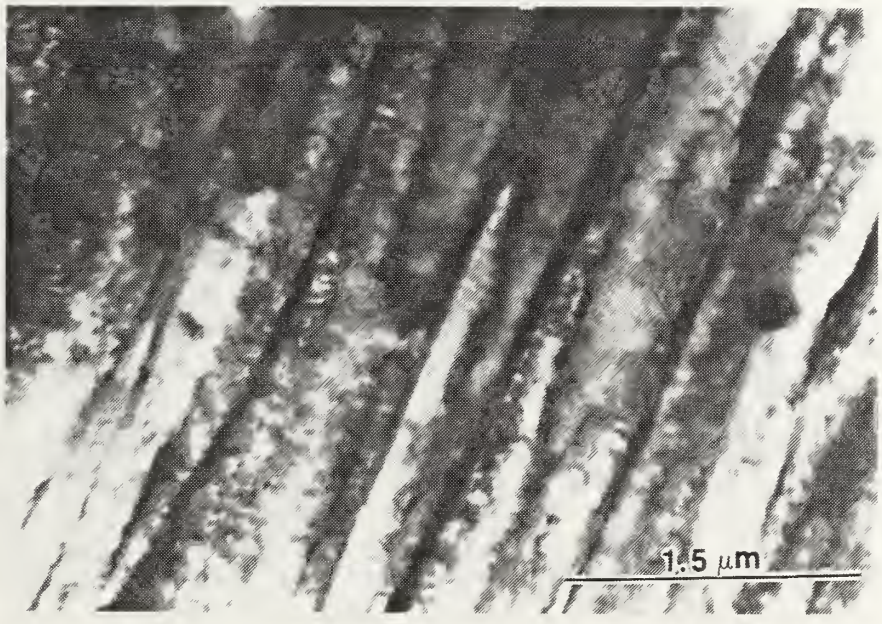

Figure 15. TEM Image Showing Lath Martensite and Retained Austenite at Lath Boundaries

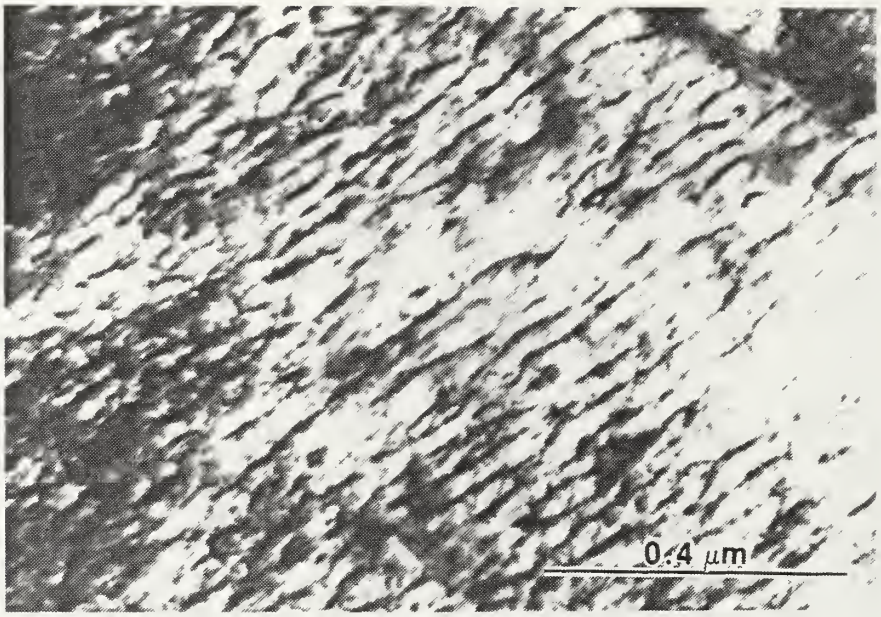

Figure 16. TEM Image Showing Bainite Lath, Dislocation and Auto Tempered Carbides

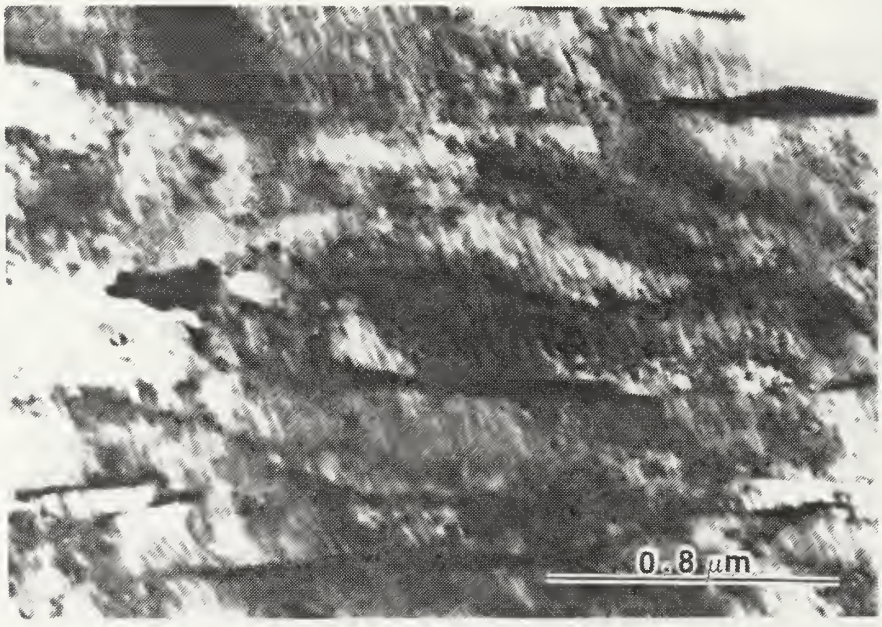

Figure 17. TEM Image Showing Blocky Retained Austenite and Bainite

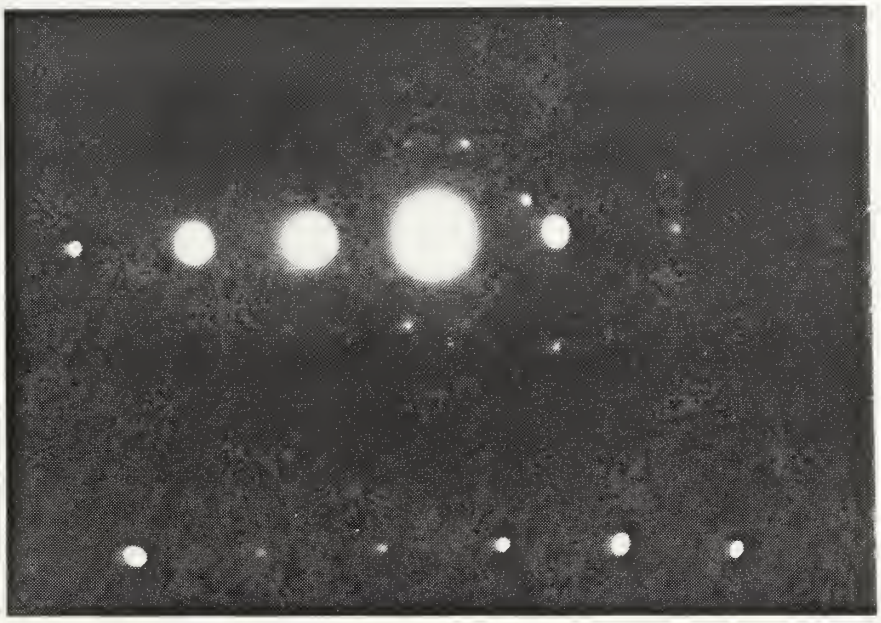

Figure 18. Diffraction Pattern Showing a [133] Crystallographic Zone Axis (Note the faint spots attributed to Fe_3C precipitates.)

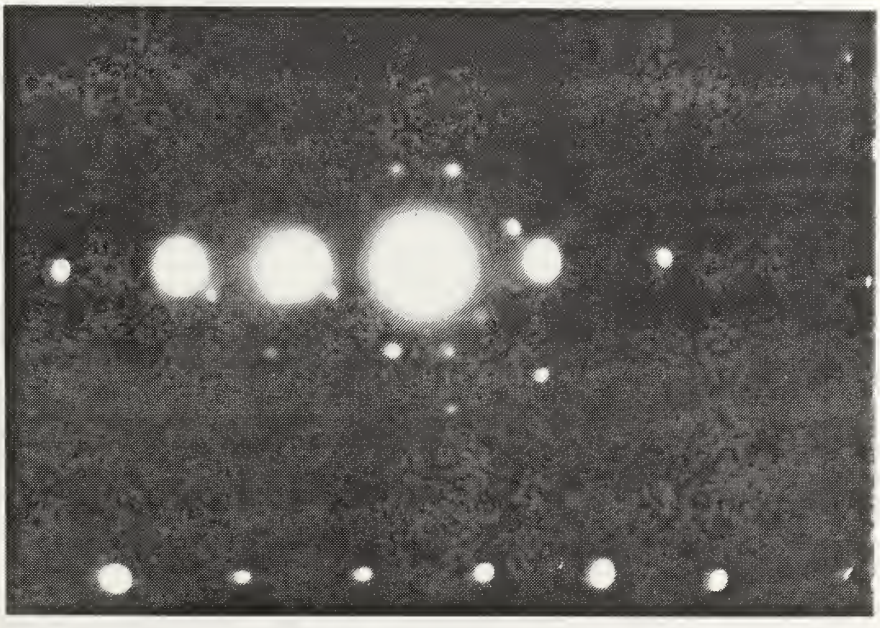

Figure 19. Diffraction Pattern Showing a [133] Crystallographic Zone Axis (Note the faint spots attributed to Fe_3C precipitates.)

2. 583°C (Peak) Aged High Copper HSLA-100 Steel

The microstructure of 538°C high copper HSLA-100 steel that had been aged one hour was observed by the optical microscope, SEM and TEM. Figures 20 and 21 are optical and SEM micrographs of the center of the "bar" sample. The samples produced a slightly larger transformation packet when compared to the as-quenched specimens. These packets consist of tempered lath martensite and bainite, retained austenite and $(FeM)_3C$ carbides. The general microstructure of the tempered lath martensite is shown in Figure 22. The width of lath is slightly larger than those in the as-quenched condition. Carbides precipitating on dislocations were also observed. Those carbide precipitates are larger than the auto-tempered carbide in the as-quenched condition. The precipitation is shown in Figure 23. The diffraction pattern associated with the carbides is presented in Figure 24. A twin-like structure was also observed; Figures 25 and 26 show the twin-like structure and diffraction pattern. Coherent BCC copper precipitates are not visible but are present.

An austenite structure will be induced to form a martensite structure when subjected to shear stress. Under conditions of rapid cooling, however, the nucleus of the martensite structure will be surrounded by an accumulation of retained austenite inhibiting the free growth of the structure. As a means of accommodating the external inhibition, dislocation will occur resulting in the formation of twins if the carbon content of the retained austenite is greater than 0.4 wt %. [Ref. 27:p. 169] This means that significant carbon segregation takes place during the quenching of the HSLA-100 steel.

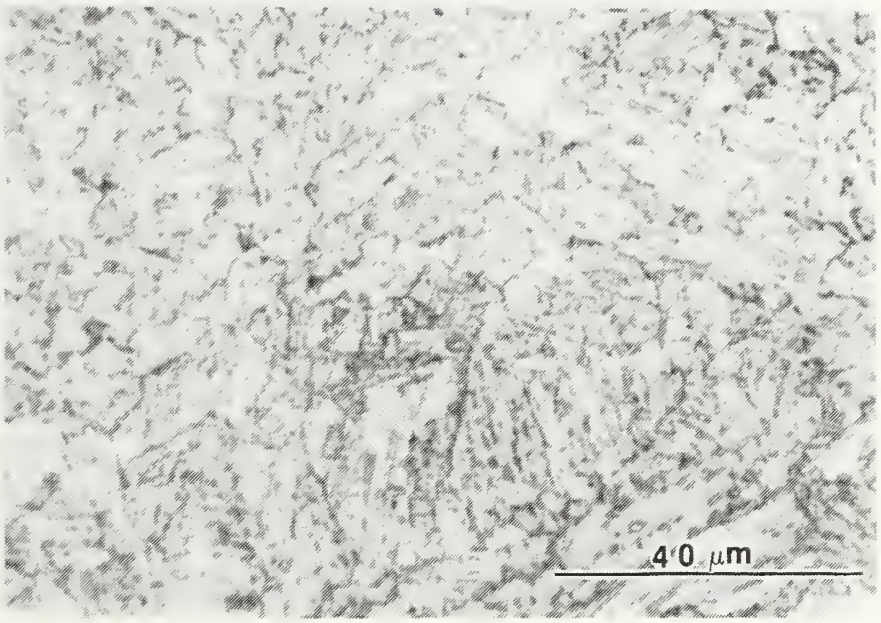

Figure 20. Optical Micrograph of 538°C Aged Transformation Product Packets

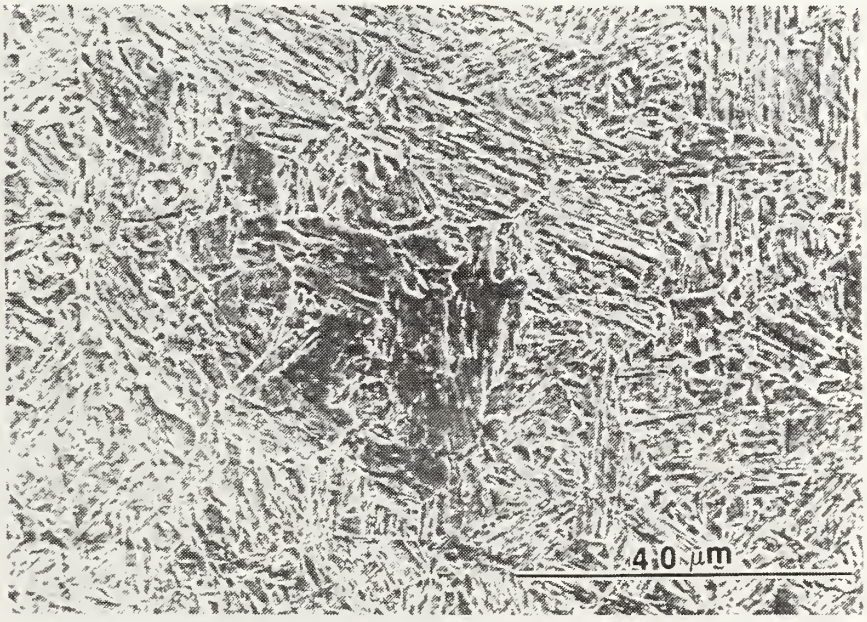

Figure 21. SEM Micrograph of 538°C Aged Transformation Product Packets

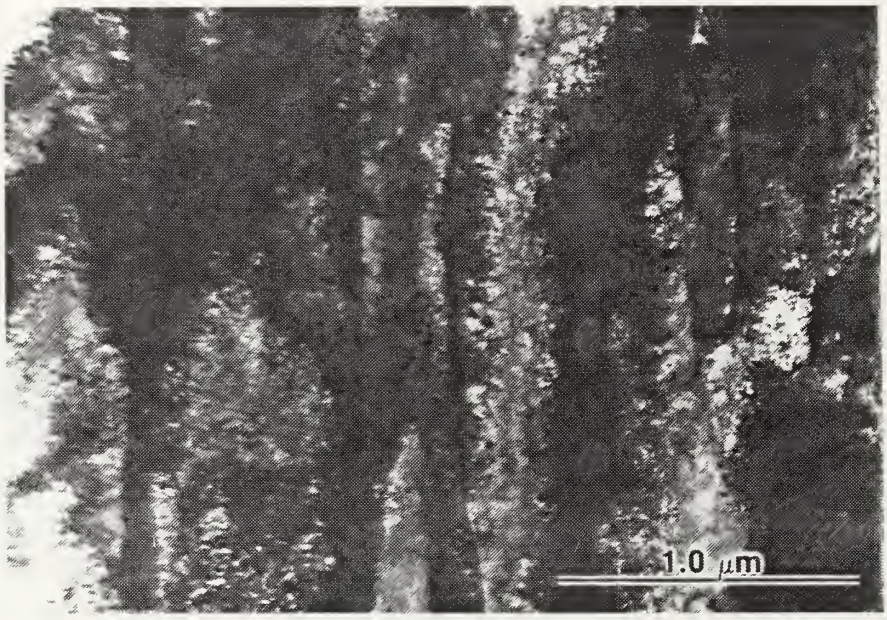

Figure 22. TEM Image Showing Tempered Lath Martensite Microstructure

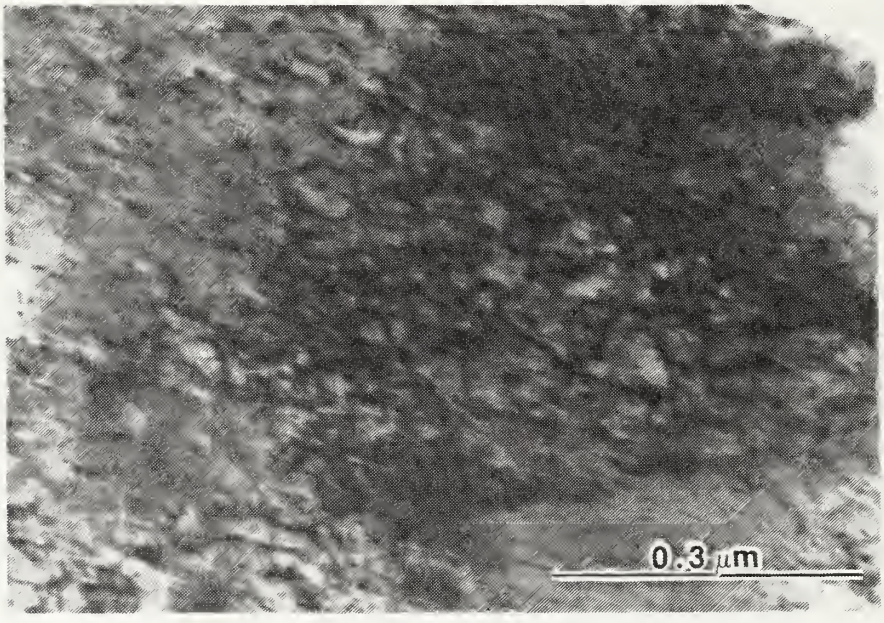

Figure 23. TEM Image Showing Tempered Fe_3C Precipitates Decorating Dislocations

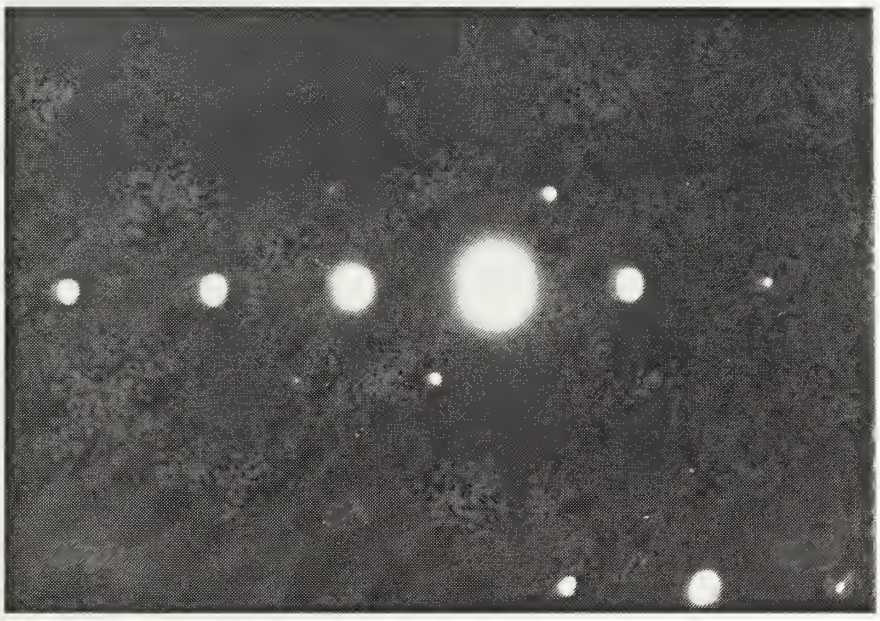

Figure 24. Diffraction Pattern Showing a [133] Crystallographic Zone Axis
(Note that there are faint spots due to the Fe_3C Precipitates.)

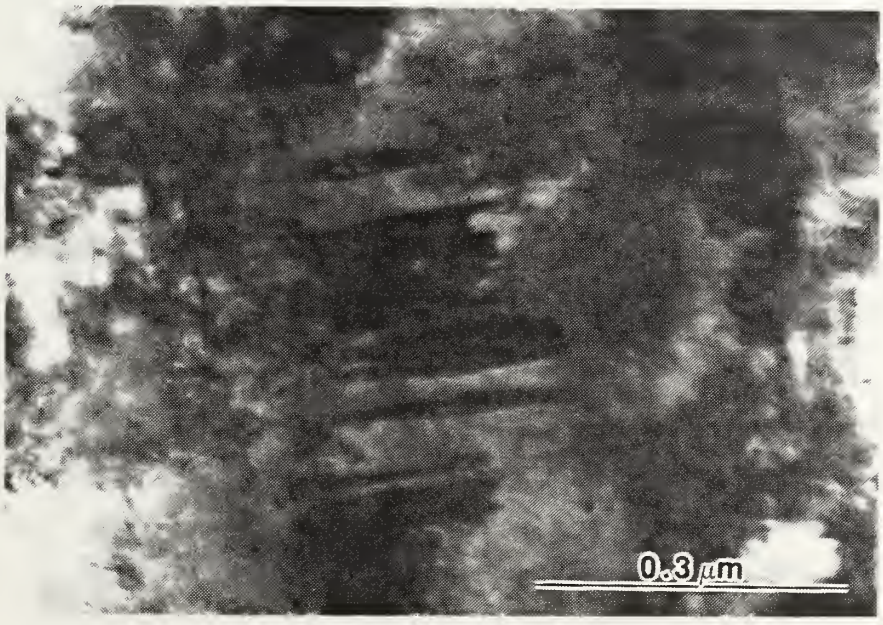

Figure 25. TEM Image Showing Twin-like Structure

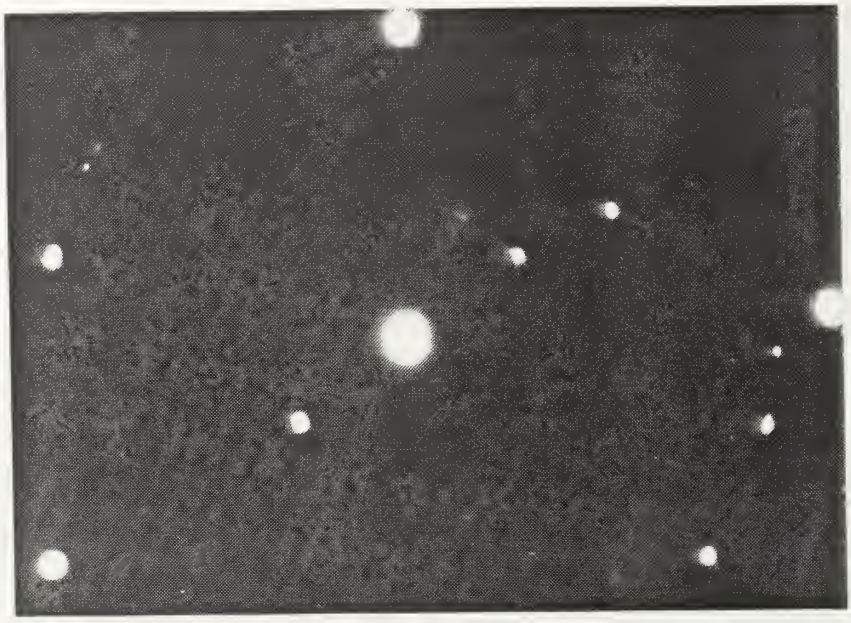

Figure 26. Diffraction Pattern Showing a Twin-like Crystallographic Zone

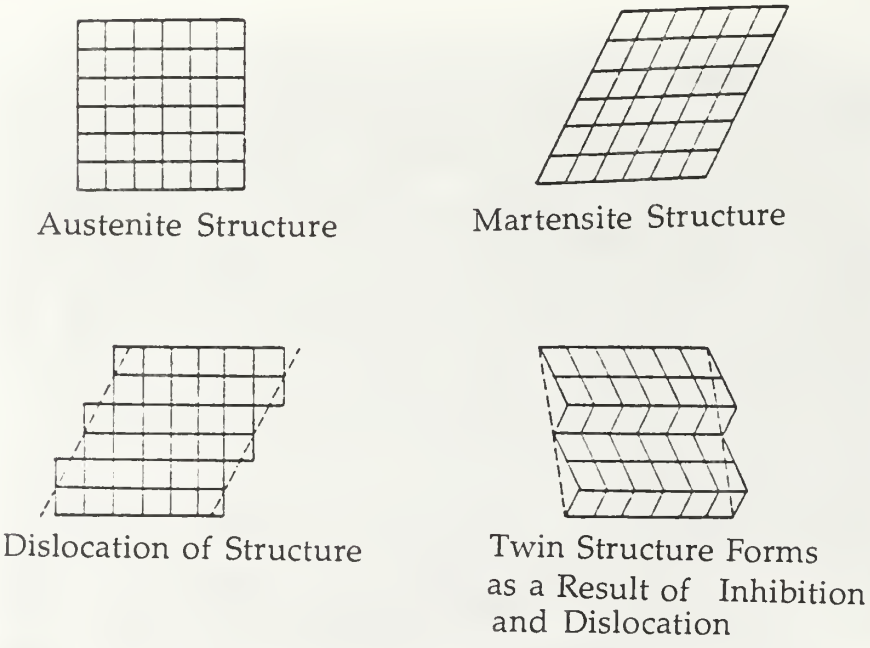

Figure 27. Mechanism of Martensite Transformation

In the 0.2% yield strength test, the sample which had undergone the 538°C heat treatment indicated the most positive values. The indications of greatest strength resulted from the effects of

- solid solution strengthening
- high dislocation density
- re-ordering of interstitial carbon atoms by aging (aging generates Cottrell atmosphere)
- Coherent precipitates of copper by tempering [Ref. 17:p. 67]

3. 593°C Aged High Copper HSLA-100 Steel

The microstructure of 593°C high copper HSLA-100 steel that had been aged one hour was observed by the optical microscope, SEM and TEM. Figures 28 and 29 are optical and SEM micrographs from the center of the "bar" sample. These samples possess a microstructure indicative of over-aging. The transformation packet size is greater than that of the 538°C aged sample. Carbide and copper precipitation at dislocations was observed and the results are shown in Figures 30 and 31. The diffraction pattern is represented in Figure 32.

The diffraction pattern shows that the precipitates that exist in the microstructure are incoherent fcc ε copper and carbides. The 0.2% yield strength is slightly below the strength requirement of HY-130 steel (130 KSI). The reduction in strength resulted from the following factors.

- The growth of copper precipitates and their incoherence with the steel matrix.
- larger transformation product packet size.
- larger lath size (lath width).

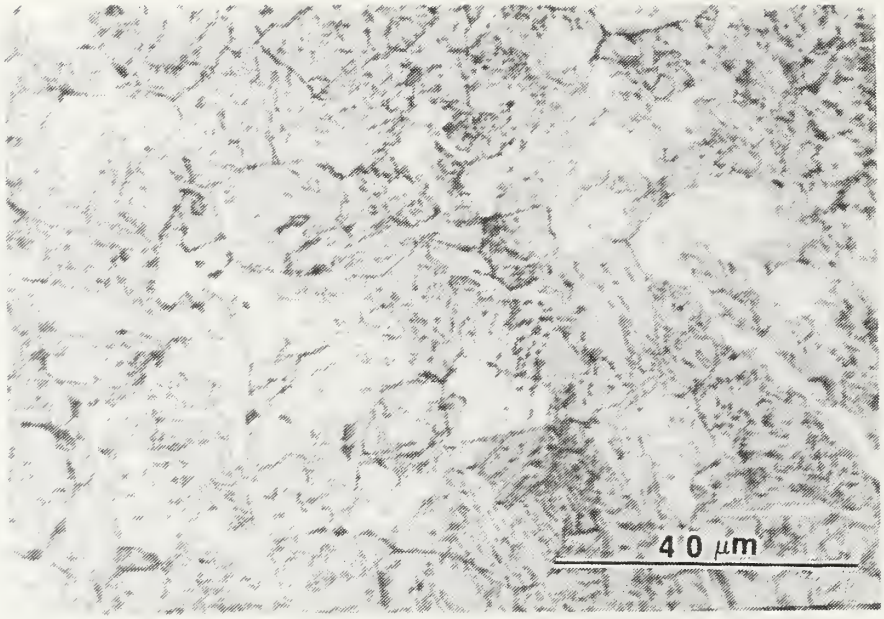

Figure 28. Optical Micrograph of 593°C Aged Transformation Product Packets

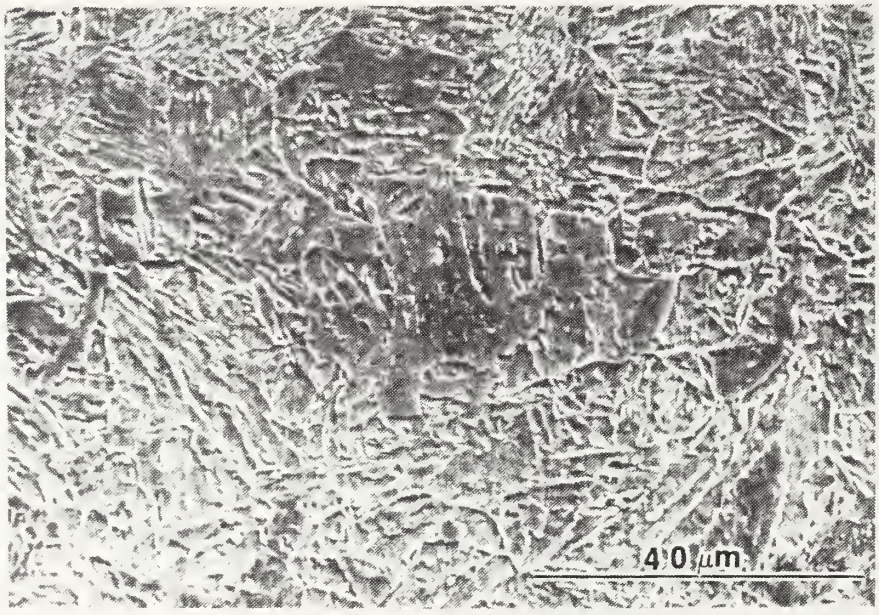

Figure 29. SEM Micrograph of 593°C Aged Transformation Product Packets

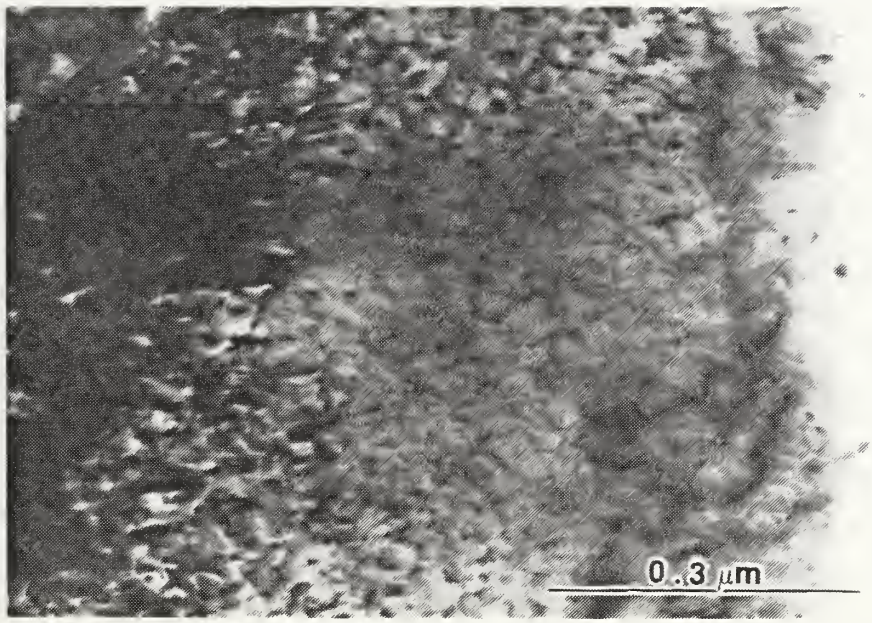

Figure 30. TEM Image Showing Incoherent fcc Copper Precipitates Decorating Dislocation (Bright Field)

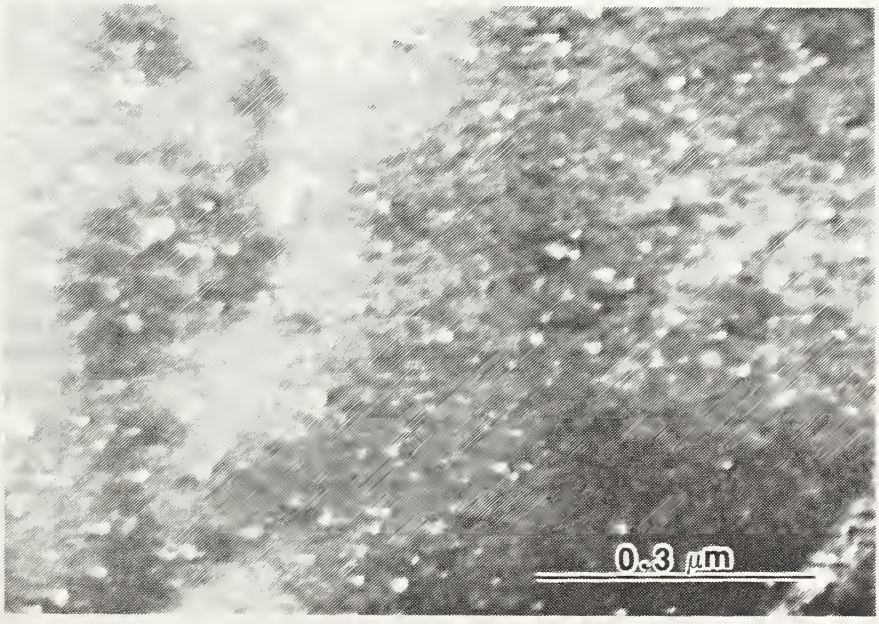

Figure 31. TEM Image Showing Incoherent fcc Copper Precipitates Decorating Dislocation (Dark Field)

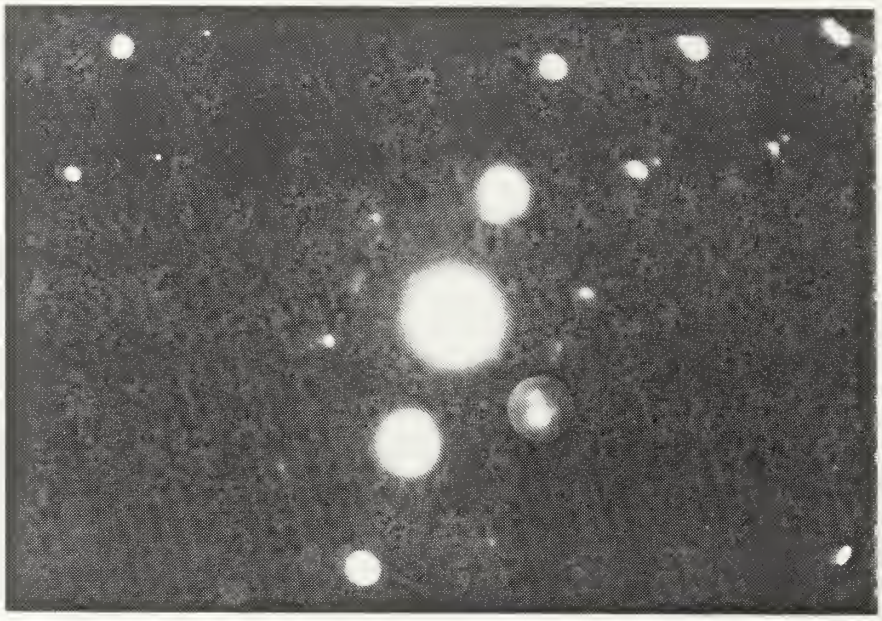

Figure 32. Diffraction Pattern of [111] Pole Showing Evidence of $(FeM)_3C$ Type Carbide

- Recovery of the dislocation substructures. [Ref. 16:p. 55] and [Ref. 28:p. 62]

4. 621°C (Over) Aged High Copper HSLA-100 Steel

The microstructure of the 621°C aged sample was very similar to the 593°C aged but the carbides and ε-Cu precipitates were somewhat larger.

The toughness of this sample increased (indicating a toughness 1.5 times greater than the toughness of a sample of the peak aged condition. The origin of this high toughness is not yet clear.

5. Transformation Product Packet Dimensions

Figure 33 shows the growth of transformation product packet size in specimens taken from the surface and center of the "block" sample. these sizes increase as aging temperature increases and the size of the center is

greater than that of the surface. The difference results from variations in the cooling rate. The cooling rate of the surface is faster than the center. In the surface region, the fraction of nucleation is greater than it is in the center.

Figure 34 shows the growth of lath width in a specimen taken from the center of the "block" sample. The dimension are closely associated with the mechanical properties. Fine packets result in a stronger microstructure. Also the short width of the lath results in a stronger microstructure that enhances yield strength. The width increases as aging temperature increases. The trend of increase is the same as the result obtained in the experiment that used 19mm plate.

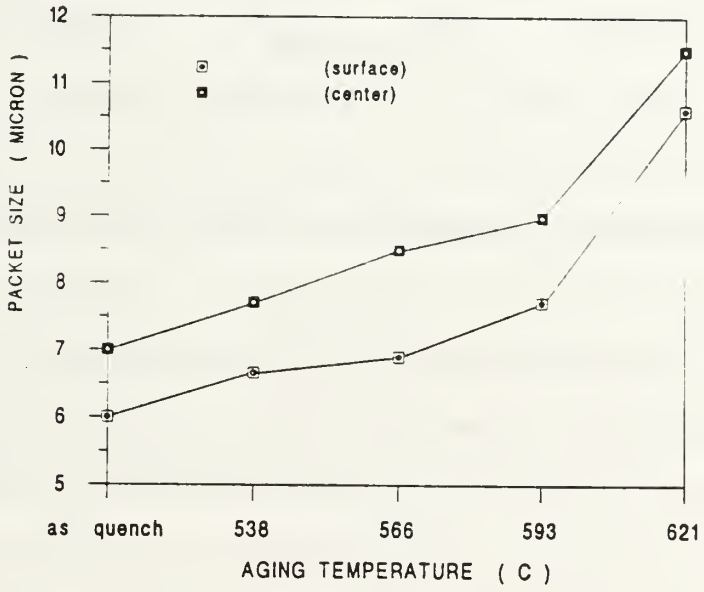

Figure 33. Variation of Transformation Product Packet Size with Aging Temperature

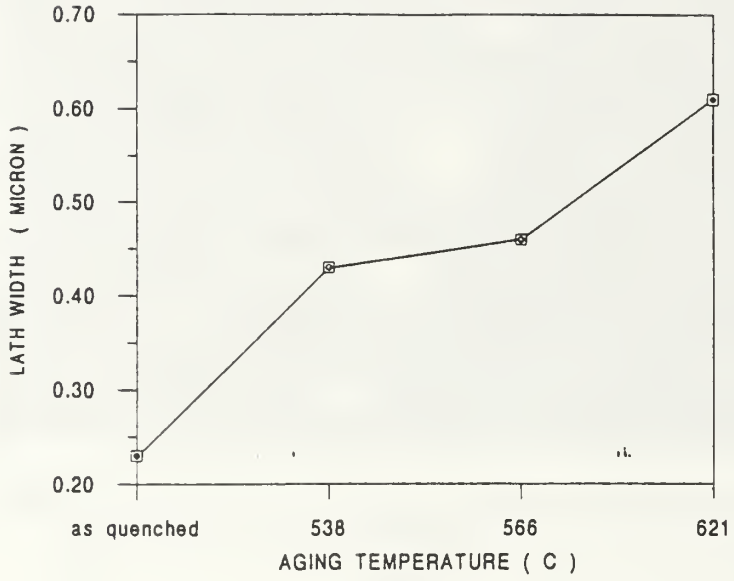

Figure 34. Variation of Martensite Lath Width with Aging Temperature

V. SUMMARY

A. CONCLUSIONS

1. Mechanical Properties

All the samples of GLE, which had differing heat treatment, satisfy the minimum requirement for strength, toughness and ductility for HSLA-100. The best combination of strength, toughness, and ductility for HSLA-100 were produced at the aging temperature of 538°C.

For appropriate temper, an aging temperature between 538°C and 621°C satisfied the minimum requirement for HSLA-130.

2. Microhardness

The as-quenched sample that was provided by DTRC was examined by Vickers microhardness throughout the thickness of the 50.8 mm plate. The Vickers hardness number varied depending upon the micro structure of the specific specimen. In the center of the plate the Vickers number decreased. We may conclude then that the microstructure in the center of the plate was bainitic ferrite and martensite rather than pure martensite. The microhardness of each sample taken from the center of the plate was also examined in regard to the specific aging temperature to which it was subjected. The sample which was aged at 593°C was the softest.

3. Microstructure

There are numerous microstructural mechanisms involved in strengthening high copper HSLA-100 steel. The mechanical properties have a very strong relationship with the mechanical structure. Three kinds of

samples, as -quenched, peak aged (538°C) and over-aged (593°C and 621°C) samples were studied in detail. In the as-quenched condition, the microstructure consists of granular bainite, lath martensite and retained austenite. The primary strengthening mechanisms are as follows:

- small transformation product packet size
- highly dislocated martensitic microstructure
- solid solution strengthening

In the 538°C aged condition, the microstructure consists of a tempered bainite/martensite microstructure with coherent copper precipitates and carbide precipitation.

The primary strengthening mechanism in this condition over and above the as-quenched condition is related to the precipitation of small coherent BCC copper precipitates.

In the 593°C and 621°C aged condition, the coherent copper precipitates change to incoherent fcc copper precipitates, causing a decrease in strength. The presence of interlath carbides, recovery of the dislocation, and ductile copper particles result in an increase of toughness.

The microstructures formed with the variations in heat treatment are consistent with the HSLA-100 CCT diagram but proeutectoid ferrite (PF) was not observed in the sample. The increased copper of HSLA-100 steel had apparently moved the proeutectoid ferrite start line to longer reaction times.

B. RECOMMENDATIONS

The following are recommended:

- Further investigation of a sample which has been aged between 566°C and 593°C would broaden the scope of understanding in the specific

relation between mechanical properties and the increase in strength and toughness.

- Investigation of samples with a wider range of variation in the copper content and the variation of mechanical properties and microstructure resulting from the variation in copper percentage.
- Investigation of the role of precipitated carbides in the strength and toughness mechanisms, i.e., study of the size, chemical composition and distribution of the carbide precipitates.

APPENDIX

TABLE A-1. DTRC CHARPY V-NOTCH IMPACT ENERGY TEST DATA
HIGH COPPER HSLA-100
DTRC CODE GLE: AS-QUENCHED CONDITION

Specimen No.	Test Temperature (°F)	Impact Energy (Ft·lb)
9	Room Temperature	90
10	"	106
11	"	116
25	"	100
26	"	86
27	"	82
12	0	96
13	0	82
14	0	96
28	0	86
29	0	88
30	0	85
15	−40	79
16	−40	70
17	−40	97
31	−40	77
32	−40	65
33	−40	78
18	−80	65
19	−80	70
20	−80	70
34	−80	62
35	−80	61
36	−80	47
21	−120	54
22	−120	55
23	−120	59
37	−120	59
38	−120	46
39	−120	44

TABLE A-2. DTRC CHARPY V-NOTCH IMPACT ENERGY TEST DATA
HIGH COPPER HSLA-100
DTRC CODE GLE: AGING TEMPERATURE 538°C

Specimen No.	Test Temperature (°F)	Impact Energy (Ft·lb)
13	Room Temperature	106
14	"	108
15	"	104
16	0	88
17	0	93
18	0	90
19	−40	92
20	−40	83
21	−40	89
22	−80	50
23	−80	50
24	−80	64
25	−120	34
26	−120	43
27	−120	35

TABLE A-3. DTRC CHARPY V-NOTCH IMPACT ENERGY TEST DATA
HIGH COPPER HSLA-100
DTRC CODE GLE: AGING TEMPERATURE 566°C

Specimen No.	Test Temperature (°F)	Impact Energy (Ft·lb)
29	Room Temperature	111
30	"	110
31	"	110
32	0	104
33	0	98
34	0	104
35	−40	82
36	−40	88
37	−40	88
38	−80	50
39	−80	54
40	−80	58
41	−120	38
42	−120	35
43	−120	44

TABLE A-4. DTRC CHARPY V-NOTCH IMPACT ENERGY TEST DATA
HIGH COPPER HSLA-100
DTRC CODE GLE: AGING TEMPERATURE 566°C

Specimen No.	Test Temperature (°F)	Impact Energy (Ft·lb)
45	Room Temperature	146
46	"	131
47	"	129
48	0	117
49	0	125
50	0	122
51	–40	115
52	–40	115
53	–40	118
54	–80	88
55	–80	106
56	–80	86
57	–120	77
58	–120	73
59	–120	70

TABLE A-5. DTRC CHARPY V-NOTCH IMPACT ENERGY TEST DATA
HIGH COPPER HSLA-100
DTRC CODE GLE: AGING TEMPERATURE 566°C

Specimen No.	Test Temperature (°F)	Impact Energy (Ft·lb)
61	Room Temperature	143
62	"	133
63	"	135
64	0	128
65	0	140
66	0	130
67	–40	130
68	–40	121
69	–40	129
70	–80	116
71	–80	109
72	–80	117
73	–120	88
74	–120	94
75	–120	88

REFERENCES

1. Pickering, F. B., *Physical Metallurgy and the Design of Steels,* Applied Science Publishers, London, 1978.

2. Czyryca, E. J., "Development of Low-carbon, Copper-strengthened HSLA Steel Plate for Naval Ship Construction, June 1990.

3. Montemarano and others, "High Strength Low Alloy Steels in Naval Construction," *Journal of Ship Production,* v. 2, n. 3, August 1986.

4. Czyryca, E. J., and others, "Development and Certification of HSLA-100 Steel for Naval Ship Construction," *Naval Engineers Journal,* May 1990.

5. Hamburg, E. G., and Wilson, A. D., "Production and Properties of Copper Aged Hardened Steels," *Processing Microstructure and Properties of HSLA Steels,* ed. A. J. Deardo, The Minerals, Metals & Materials Society, 1988.

6. Gudas, J. P., *Pre-certification Development Plan—HSLA-130 for Submarine Construction,* David Taylor Research Center, Metals and Welding Division, Annapolis, March, 1989.

7. Mohr, T. C., *A Study of the Microstructural Basis for the Strength and Toughness Properties of Water Quenched and Air Cooled HSLA-100, HSLA-100 with Increased Copper and a ULCB Steel,*" Master's Thesis, Naval Postgraduate School, Monterey, CA, September 1991.

8. Garcia, C. I., Lis, A. K., Deardo, A. J., *The Physical Metallurgy of Ultra-low Carbon Bainitic Plate Steels,* University of Pittsburgh, 1990.

9. Graville, B. A., *Proceeding Welding of HSLA (Microalloyed) Structural Steels (Roms),* Metals Park, 1978.

10. Bucher, J. H., E. G. Hamburg, and A. D. Wilson, *Symposium on Toughness Characterization and Specification for HSLA and Structural Steels,* The Metallurgical Society of AIME, March 1977.

11. Coldren, A. P. and Cox, T. B., *Development of 100 KSI Yield Strength HSLA Steel,* DTNSRDC/SME-CR-07-86, July 1976.

12. Czyryca, E. J., Link R. E., *Physical Properties, Elastic Constants, and Metallurgy*, DTIC Selecte, April 11, 1989.

13. Wilson, A. D. and others, "Properties and Microstructures of Copper Precipitation Aged Plate Steels, Microalloyed HSLA Steels," *Proceedings of Microalloying '88,*, ASM International.

14. *Marks' Mechanical Engineers' Handbook, Sixth Edition*, T. Baumeister, editor, McGraw-Hill, 1958.

15. "The Role of Copper in HSLA Steels: a Review and Update, May, A, Schetky, L. M., and Krishnadov, M. R., in *Proceedings of an International Conference*, University of Wollongong, August 1984.

16. Harvey, A. W., *A Study of the Microstructural Basis for the Strength and Toughness Properties of As-Quenched and Quenched and Tempered High Copper HSLA-100 Steel*, Master's Thesis, Naval Postgraduate School, Monterey, CA, December 1991.

17. Richman, M. H., *An Introduction to the Science of Metals*, Ginn Custom Publishing, 1974.

18. LeMay, I, and Schetky, L. M., *Copper in Iron and Steel*, John Wiley and Sons, New York, 1982.

19. Ruoft, A. L., *Materials Science*, Prentice-Hall, Inc., England Cliffs, 1973.

20 Pascoe, K. J., *An Introduction to the Properties of Engineering Materials*, Van Nostrand Reinhold Company, London, 1972.

21. Grossmann, M. A. and E. C. Bain, *Principles of Heat Treatment, Fifth Edition*, American Society for Metals, Metals Park, 1964.

22. Chilton, J. M. and P. M. Kelly, "The Strength of Ferrous Martensite," *Acta Metallurgica*, v. 16, May 1968.

23. Aborn, R. H., "Low Carbon Martensites," *Transactions of the ASM*, v. 48, 1956.

24. Speich, G. R., "Tempering of Low Carbon Martensite," *Transactions of the ASM*, v. 245, December 1969.

25. Mikalac, S., *Private Communication*, 1992.

26. Comerford, L. W. *A Study of the Microstructural Basis for the Strength and Toughness Properties of the Over-ages HSLA-100 Steel,* Master's Thesis, Naval Postgraduate School, Monterey, CA, June 1991.

27. Thoru A., *Metallurgy of Steel*, Maruzen, Tokyo, 1970.

28. Mattes V. R., *Microstructure and Mechanical Properties of HSLA-100 Steel*, Master's Thesis, Naval Postgraduate School, Monterey, CA, December, 1990.

INITIAL DISTRIBUTION LIST

1. Library (Code 52) 2
   Naval Postgraduate School
   Monterey, CA 93943-5000

2. Defense Technical Information Center 2
   Cameron Station
   Alexandria, VA 22314

3. Code ME/Hy 1
   Department of Mechanical Engineering
   Naval Postgraduate School
   Monterey, CA 93943-5000

4. Naval Engineering Curricular Office, Code 34 1
   Naval Postgraduate School
   Monterey, CA 93943-5000

5. Code ME/Fx 1
   Department of Mechanical Engineering
   Naval Postgraduate School
   Monterey, CA 93943-5000

6. Chairman 1
   Department of Mechanical Engineering
   National Defense Academy
   1-10-20 Hashirimizu, Yokosuka, Japan
   239

7. Chairman 1
   Department of Mechanical Engineering
   Nihon University, the Faculty of Technology
   1, Nakagawara, Tokusada, Tamura-Machi
   Kohriyama-Shi, Fukushima-Ken, Japan

8. LT. Suka Akira (JMSDF) 1
   Officer Candidate School
   Edazima-Chiyo, Aki-gun, Hiroshima-Ken
   737-21 JAPAN

Thesis
S858273 Suka
c.1 Microstructure and mechanical properties of high copper HSLA-100 steel in 2-inch plate form.

Thesis
S858273 Suka
c.1 Microstructure and mechanical properties of high copper HSLA-100 steel in 2-inch plate form.

AMERICAN BINDERY 2 9-83

DUDLEY KNOX LIBRARY
3 2768 00036325 3